

ISTANBUL TECHNICAL UNIVERSITY ★ GRADUATE SCHOOL OF SCIENCE
ENGINEERING AND TECHNOLOGY

**ANALYSIS AND
FIELD OBSERVATION OF
DIESEL FUEL INJECTOR NOZZLE RELIABILITY**

M.Sc. THESIS

İbrahim CİVANOĞLU

Department of Mechanical Engineering

Automotive Engineering Programme

DECEMBER 2017

ISTANBUL TECHNICAL UNIVERSITY ★ GRADUATE SCHOOL OF SCIENCE
ENGINEERING AND TECHNOLOGY

**ANALYSIS AND
FIELD OBSERVATION OF
DIESEL FUEL INJECTOR NOZZLE RELIABILITY**

M.Sc. THESIS

**İbrahim CİVANOĞLU
(503121707)**

Department of Mechanical Engineering

Automotive Engineering Programme

Thesis Advisor: Asst. Prof. Dr. Akın KUTLAR

DECEMBER 2017

İSTANBUL TEKNİK ÜNİVERSİTESİ ★ FEN BİLİMLERİ ENSTİTÜSÜ

**DİZEL ENJEKTÖR MEMESİNİN
SAHA GÜVENİLİRLİĞİNİN
İNCELENMESİ**

YÜKSEK LİSANS TEZİ

**İbrahim CİVANOĞLU
(503121707)**

Makina Mühendisliği Anabilim Dalı

Otomotiv Mühendisliği Programı

Tez Danışmanı: Yard. Doç. Dr. Akın KUTLAR

ARALIK 2017

İbrahim Civanoglu, an M.Sc. student of İTÜ Graduate School of Science Engineering and Technology student ID 503121707, successfully defended the thesis entitled “ANALYSIS AND FIELD OBSERVATION OF DIESEL FUEL INJECTOR NOZZLE RELIABILITY”, which he prepared after fulfilling the requirements specified in the associated legislations, before the jury whose signatures are below.

Thesis Advisor : **Asst. Prof. Dr. Akın KUTLAR**
İstanbul Technical University

Jury Members : **Asst. Prof. Dr. Akın KUTLAR**
İstanbul Technical University

Prof. Dr. Cemal BAYKARA
İstanbul Technical University

Prof. Dr. Muammer ÖZKAN
Yıldız Technical University

Date of Submission : 17 November 2017

Date of Defense : 14 December 2017





To my family,



FOREWORD

First and foremost, I would like to express my endless gratitude to the countless heroes and the unforgettable leader of my country, Mustafa Kemal Atatürk for all their perseverance, their selfless efforts and sacrifice for my country. It is their efforts, which gives me the chance to start and complete this study.

I would like to express my most sincere gratitudes to my family. I am forever in their debt for all they did for me.

I would like to express my special gratitudes to Asst. Prof. Funda H. Sezgin, for her contributions and valuable guidance in my study.

I have always felt privileged to be a part of the big family founded by Robert Bosch. His heritage and vision to "... always endeavour to do better." have guided me through my work life and my studies.

I thank all my colleagues and my managers Ersoy Bey, Ahmet Bingöl, and Adil Okumuşoğlu for their support in this study. I am proud to have them and to know that I can count on them whenever necessary.

Last but not least, I would like to thank my friends Onur Gezer, Merve Üngör, Kübra Erkul and Harun Topçu who supported me for this study.

November 2017

İbrahim CİVANOĞLU
(Mechanical Engineer)



TABLE OF CONTENTS

	<u>Page</u>
FOREWORD	ix
TABLE OF CONTENTS	xi
ABBREVIATIONS	xiii
SYMBOLS	xv
LIST OF TABLES	xvii
LIST OF FIGURES	xix
SUMMARY	xxi
ÖZET	xxiii
1. INTRODUCTION	1
2. DIESEL FUEL INJECTION SYSTEM	7
2.1 The Evolution of the Diesel Fuel Injection System	7
2.2 Diesel Injector Nozzle	9
3. IMPURITIES IN MATERIAL AND NOZZLE FAILURES	13
4. WEIBULL ANALYSIS	21
5. EVALUATION OF NON METALLIC INCLUSION RELATED NOZZLE FIELD FAILURE PROBABILITY	27
6. RESULTS AND CONCLUSIONS	37
REFERENCES	45
CURRICULUM VITAE	47



ABBREVIATIONS

AD	: Anderson-Darling goodness-of-fit statistic
Al	: Aluminum
Al_2O_3	: Aluminum oxide
C	: Carbon
CaO	: Calcium oxide
CI	: Confidence interval
CO	: Carbon monoxide
CO_2	: Carbon dioxide
EDX	: Energy dispersive X-ray analysis
EGR	: Exhaust gas recirculation
H	: Hydrogen
HC	: Hydrocarbon
IQR	: Interquartile range
LSXY	: Least squares estimation method
MgO	: Magnesium oxide
N	: Nitrogen
NMI	: Non-metallix inclusion
NO_x	: Nitrogen oxides
PM	: Particulate matter
S	: Sulphur
SEM	: Scanning electron microscope
SEN	: Submerged entry nozzle
StDev	: Standard deviation
T.O.	: Total oxygen
WHO	: World Health Organization



SYMBOLS

β	: Weibull shape parameter
η	: Weibull scale parameter
γ	: Weibull location parameter
t	: Time





LIST OF TABLES

	<u>Page</u>
Table 3.1 : Accepted adequate impurities and inclusion in steel products.	14
Table 5.1 : Load coefficient comparison of different designs.	34
Table 6.1 : Table of estimated Weibull distribution parameters	40





LIST OF FIGURES

	<u>Page</u>
Figure 1.1 : Change of carbon dioxide and methane with respect to years.	1
Figure 1.2 : Change of calculated temperature anomaly with respect to years	2
Figure 1.3 : Global premature deaths from light and heavy duty vehicle exhaust PM	2
Figure 1.4 : Worldwide PM 2.5 emission measurement results.	3
Figure 1.5 : Change of vehicle technical parameters with respect to years.	4
Figure 2.1 : Diesel fuel injection system development milestones.	7
Figure 2.2 : Objectives and functions related to the diesel injector nozzle.	9
Figure 2.3 : Modern diesel injector nozzle construction.	11
Figure 2.4 : Sachole design and its effects on nozzle properties.	11
Figure 3.1 : Diagram showing molten steel reoxidation.	15
Figure 3.2 : Size distribution of oxide inclusions during steady state casting and ladle change	15
Figure 3.3 : Clogging materials at the submerged entry nozzle	16
Figure 3.4 : Formation of non-metallic inclusions.	17
Figure 3.5 : Fatigue strength reduction factor vs mean inclusion diameter.	17
Figure 3.6 : Flaking life of ball bearings vs the number of oxide inclusions	18
Figure 3.7 : Fatigue life with 10% failure probability with respect to oxygen content.	18
Figure 3.8 : Inclusion forms of hard and soft inclusions before and after rolling ..	19
Figure 4.1 : Weibull probability density function with respect to β value	22
Figure 4.2 : Effect of shape parameter β on unreliability	23
Figure 4.3 : Effect of shape parameter β on reliability.	24
Figure 4.4 : Effect of shape parameter β on failure rate	24
Figure 4.5 : Weibull PDF and characteristic life	25
Figure 4.6 : Weibull PDF and scale parameter η	25
Figure 4.7 : Weibull PDF and location parameter γ	26
Figure 5.1 : Classification of nozzle failures with respect to their root cause	27
Figure 5.2 : SEM photograph of a diesel injector nozzle	28
Figure 5.3 : SEM photograph of a diesel injector nozzle	28
Figure 5.4 : SEM photograph of a diesel injector nozzle	29
Figure 5.5 : SEM photograph of a diesel injector nozzle	29
Figure 5.6 : SEM photograph of a diesel injector nozzle	30
Figure 5.7 : SEM photograph of a diesel injector nozzle	30
Figure 5.8 : SEM photograph of a diesel injector nozzle	31
Figure 5.9 : SEM photograph of a diesel injector nozzle.	31
Figure 5.10 : Field failure probability in a nozzle type in series manufacturing	32
Figure 5.11 : Positions of the NMIs which caused field failures	33
Figure 5.12 : Definition of the volume withstanding the needle closing force.	33
Figure 5.13 : Number of NMI induced nozzle tip failures per design	34
Figure 5.14 : NMI induced nozzle tip failures percentage per mileage in field	35
Figure 5.15 : Daily mileage in field per design	35

Figure 5.16 : Comparison of number of runout nozzles per design.....	36
Figure 6.1 : Weibull distribution plot for design #1.....	37
Figure 6.2 : Weibull distribution plot for design #2.....	38
Figure 6.3 : Weibull distribution plot for design #3.....	38
Figure 6.4 : Weibull distribution plot for design #4.....	39
Figure 6.5 : 3-parameter Weibull distribution plot for design #4	39
Figure 6.6 : Field failure probability vs load coefficient F/A	40
Figure 6.7 : Weibull distribution plot for 4 variants combined.....	41
Figure 6.8 : 3-parameter Weibull distribution plot for 4 variants combined	42
Figure 6.9 : Weibull distribution plot for design #5.....	42
Figure 6.10 : 3-parameter Weibull distribution plot for design #5	43



ANALYSIS AND FIELD OBSERVATION OF DIESEL INJECTOR NOZZLE RELIABILITY

SUMMARY

In this study, the field reliability of injector nozzles from common rail diesel injection systems is analyzed. In order to understand the requirements from the common rail system and the nozzle, the developments in the automotive industry and the technical requirements originating from the environmental problems and therefore the emission regulations are evaluated. Based on the injector nozzle requirements, the related injector nozzle functions are listed and the connection between field requirements and nozzle strength requirements are shown. The evolution and the milestones of diesel injection systems and the construction of modern diesel injector nozzles are covered. Modern injector nozzle design and its effects on injector nozzle strength functions are remarked.

Injector nozzle strength is also inevitably effected by the properties of the material. The nozzle material needs to have certain qualities such as high strength, wear resistance, good machinability properties, availability in large quantities and acceptable cost. The formation of impurities in the material can cause low material performance. The continuous casting process and the formation of impurities such as non-metallic inclusions are explained.

For the statistical evaluation of the nozzle field reliability, a Weibull analysis is made. The advantage of using Weibull distribution for the field reliability analysis and its typical application areas are given. The characteristic parameters defining the shape of the Weibull distribution plots and the effect of these parameters on the probability density function, failure rate, reliability and unreliability characteristics are covered. are explained.

In order to evaluate the field reliability properties of the diesel injector nozzle, the data from the field is sorted and organized. Properties such as the spray design, nozzle tip geometry, manufacturing date non-metallic inclusion type and dimensions, the positions of the found impurities, failure mileage and customer are used as criteria for organizing the failure data. The main causes found for field failures are listed. It is seen that the majority of the field reliability problems are linked to non-metallic inclusions. Different shapes and types of inclusions are given as examples. Based on the manufacturing date of failed nozzles, it is shown that the failures due to impurities are not due to a problem with a single steel melting batch. The positions of the impurities causing failures from the nozzle tip are shown. Based on the field loads acting on the nozzle tip, the positions of the failure causing impurities and the design properties effecting the nozzle tip strength, a load coefficient is defined. Based on the failure data from the field, the mileage until which almost all failures originating from non-metallic inclusions occur is found. The daily mileage for each nozzle design in field is given. The relevant nozzle manufacturing volume which already covered the critical mileage is found. Using the number of failures and the number of runout nozzles in field, the failure data and the suspensions which will be the inputs for the Weibull analysis are

found. Using Minitab software, the Weibull plot for the field reliability of four different designs are plotted. Based on these plots, it is discussed, whether the distribution represents the field data correctly. Based on the estimated parameters, a discussion is made over whether the estimated parameters and the load coefficient of nozzle tip design have a correlation. It is concluded that due to very low field failure probability and hence scarce data related to failures, the parameters could not be estimated very accurately and therefore a direct correlation of Weibull parameters could not be found. However, the failure probability of these four designs and the load coefficient show an exponential correlation and therefore may indicate that with more data, the Weibull distribution could prove adequate for the analysis of non-metallic inclusion related injector nozzle tip failures.

In order to search for a correlation between the field experience and the estimated Weibull distribution parameters from a different perspective, the combined field character of the previously compared four designs is analyzed. The results and the estimated Weibull distribution parameters are then compared to that of a fifth design. Comparison and analysis of field data related to the first 4 designs combined and the 5th showed that because of very few failures in field resulting in very small failure probability and therefore scarce data related to failures, the parameters could not be estimated very accurately, as a result of which a direct prediction of Weibull parameters was not possible. However, it was found the estimated shape factors for other designs combined and the 5th design did not show a very high variance, indicating that the Weibull distribution could prove adequate to analyze and predict non-metallic inclusion related injector nozzle tip failures seen in field.

DİZEL ENJEKTÖR MEMESİNİN SAHA GÜVENİLİRLİĞİNİN İNCELENMESİ

ÖZET

Bu çalışmada, dizel motorlarının yakıt püskürtme sistemlerinde kullanılan enjektör memelerinin saha güvenilirliği incelenmiştir. Dizel yakıt püskürtme sistemi ve enjektör memesinin karşılaması gereken beklentileri anlayabilmek için, çevresel problemler, bu problemlerin önüne geçmek üzere hazırlanan emisyon regülasyonları ve otomotiv endüstrisindeki genel eğilim değerlendirilmiştir.

Atmosferdeki sera gazlarının miktarı sanayi devriminden bu yana hızlanarak artmaktadır ve bu durum küresel ortalama yüzey sıcaklıklarının giderek artmasına yol açmaktadır. Motorlu taşıt kaynaklı kirletici emisyonların insan sağlığına ve çevreye etkisini azaltmak amacıyla emisyon standartları güncellenmekte ve eksoz gazı emisyonlarının kontrol altında tutulması için yakıt enjeksiyon sistemlerinin karşılaması gereken teknik gereklilikler de giderek artmaktadır. Bu gereklilikleri karşılamak için dizel enjektör memesinin sağlaması gereken fonksiyonlar listelenmiş ve saha gereklilikleri ile enjektör memesinin dayanım özellikleri arasındaki bağlantı gösterilmiştir.

Dizel motorlarında kullanılan yakıt püskürtme sistemlerinin gelişimi ve bu gelişimin kilometre taşlarının üzerinden geçilmiş ve dizel enjektör memesinin konstrüksiyonuna değinilmiştir. Taşıtların emisyon standartlarına uyumluluk gösterebilmesi için giderek daha düşük kirletici emisyon çıktısı üretmesi gerekmektedir. Bu gerekliliği karşılamak amacıyla, yanma odası içerisindeki havanın daha etkin şekilde kullanımı ve hava-yakıt karışımının daha homojen şekilde sağlanması gerekmektedir. Bu durum dizel yakıt enjeksiyon sistemi tarafından giderek daha yüksek püskürtme basınçlarının sağlanması gerekliliğini ortaya çıkarmıştır. Yüksek sistem basıncı nedeni ile enjektör memesinin sahada karşılaştığı yükler giderek yükselmiştir. Bu gereklilikler ışığında modern enjektör memesi tasarımının gelişimi ve tasarım özelliklerinin kubbe dayanımına olan etkisinden bahsedilmiştir.

Enjektör memesinin dayanım özellikleri kaçınılmaz olarak malzeme özelliklerinden de etkilenmektedir. Meme malzemesinin yüksek mukavemet, yüksek aşınma dayanımı, kolay işlenebilirlik, yüksek miktarlarda temin edilebilirlik ve düşük maliyet gibi özelliklere sahip olması gerekmektedir.

Malzeme içerisinde oluşan safsızlıklar malzemenin düşük performans göstermesine sebebiyet verebilmektedir. Sürekli döküm tekniği ile çelik üretimi ve dayanım düşüşüne neden olan endojen ve eksojen metal dışı safsızlıklardan bahsedilmiş, bu safsızlıkların alt sınıflandırmalarına değinilmiştir. Oksit ve sülfid inklüzyonlarının oluşum yollarından ve sürekli döküm prosesi sırasında bu inklüzyonların sayılarının arttığı ve boyutlarının yükseldiği durumlardan söz edilmiştir.

Metal dışı inklüzyonların çelik kalitesine doğrudan ve dolaylı etkileri bulunmaktadır. Safsızlıkların çelik yapısına doğrudan etkileri, malzemenin dayanım özelliklerinde gözlemlenmektedir. Dolaylı etkilerden biri ise döküm memesinin tıkanması

durumunda kalite düşüşü ve bazı durumlarda sürekli dökümün durma noktasına gelmesi olmaktadır. Büyük boyutlardaki safsızlıklara daha nadir rastlanırken, daha küçük boyutlu safsızlıklarla daha sık karşılaşılmaktadır.

Çelik içerisinde oksit ve sülfür miktarının artışı, çeliğin sünekliği ve kırılma tokluğu üzerinde negatif bir etkiye sahip olmaktadır. Kritik boyutun üzerindeki inklüzyonların sayısı ve kritik miktarın üzerinde oksit içeriği, ürünün ömrünü kısaltmaktadır.

Inklüzyonların sertlikleri, plastik şekil verme işlemleri sonrasında inklüzyonun geleceği şekle ve dolayısıyla neden olacağı çentik etkisi ve dayanım düşüşüne etki etmektedir.

Çelik içerisindeki inklüzyonların tespiti için çeşitli yöntemlerden faydalanılmaktadır. Bu yöntemlerden bazıları seri üretim koşullarına uyarlanabilmiştir ve çelik üretiminde kalite kontrol amaçlı kullanılmaktadır. Bu amaçla faydalanılan ve kabul gören yöntemlerde çeliğin oksidik ve sülfürik safsızlıklar bakımından mikroskopik düzeydeki arılığı ve makroskopik inklüzyonların varlığı ve boyutları kontrol edilmektedir.

Enjektör memesinin saha güvenilirliğinin incelenmesinde Weibull analizinden faydalanılmıştır. Weibull analizinin esneklik, sınırlı hata verisine dayanarak makul tahminler üretilmesine imkan sağlama, dağılım parametrelerine bağlı olarak diğer dağılımlar gibi davranma, hata oranının zamana göre değiştiği durumları modelleyebilme gibi avantajlarından bahsedilmiştir. Weibull analizinden elektron tüpleri, röleler, bilyalı yatakların saha performansının modellenmesi, hava durumu ve rüzgar hızı tahminleri gibi pek çok alanda faydalanılmaktadır. Weibull dağılımı grafiklerinin şeklini belirleyen karakteristik parametreler ve bunların olasılık yoğunluk fonksiyonu, güvenilirlik, hata oluşum sıklığına etkisi açıklanmıştır.

Dizel yakıt enjektörü memesinin saha güvenilirlik özelliklerinin incelenmesi için, öncelikle sahadan gelen bilginin düzenlenmesi ve doğru şekilde sınıflandırılması gerekmektedir. Bu amaçla enjektör memesine dair sahadan gelen bilgiler ve hatanın görüldüğü enjektör memesinin püskürtme sprej geometrisi, kubbe bölgesinin tasarımı, üretim tarihi, eğer bulundu ise safsızlıkların çeşidi, boyutları ve meme gövdesi üzerindeki pozisyonları, hata oluşmadan evvel sahada kat edilen mesafe ve müşteri bilgileri, hataların sınıflandırılması ve düzenlenmesinde birer kriter olarak kullanılmıştır.

Çalışmada, enjektör memesinin kubbe bölgesinden çatlaması hata olarak tanımlanmıştır. Hata oluşumuna neden olan ana nedenler listelenmiştir. Bu bilgilere göre sahada gözlemlenen hataların çoğunluğunun metal dışı safsızlıklardan kaynaklandığı görülmüştür. Değişik tip ve şekildeki safsızlıklar örnek olarak gösterilmiştir.

Hata yaşanan enjektör memelerinin üretim tarihleri ve hata oranları incelendiğinde, metal dışı safsızlıklardan kaynaklanan hataların tek bir çelik döküm şarjına ait olmadığı ve dolayısıyla benzer safsızlıkların çelik üretiminde belirli bir tarih aralığında değil, üretim prosesinin bir yan ürünü olarak oluştuğu gözlemlenmiştir.

Sahada hataya sebebiyet veren safsızlıkların meme gövdesi üzerindeki pozisyonları gösterilmiştir. Memenin kubbe bölgesine sahada etki eden yükler, hataya sebep olan safsızlıkların pozisyonları, ve memenin kubbe dayanımına etki eden tasarım parametreleri göz önünde bulundurularak, değişik tasarımların karşılaştırılmasında kullanılabilecek bir "yük katsayısı" tanımlanmıştır.

Sahadan elde edilen hatalı parça bilgilerinden yola çıkılarak, metal dışı safsızlıklardan kaynaklanan hataların tamamına yakını ortaya çıkmadan önce ilgili araçlar tarafından sahada kat edilen mesafe belirlenmiştir. Yine hatalı parça bilgilerinden yola çıkılarak, karşılaştırmada kullanılan her bir tasarımın üretim tarihinden itibaren bir günde kat ettikleri ortalama mesafe hesaplanmıştır. Bu bilgilerden faydalanılarak, karşılaştırması yapılacak her bir tasarım için sahada hataların tamamının ortaya çıkacağı kritik mesafeyi kat etmiş olan enjektör memelerinin sayısı bulunmuştur. Her bir tasarım için hata sayısı ve sahada kritik mesafeyi aşmış olan parça sayısı Weibull analizinde birer girdi olarak kullanılmıştır.

Weibull dağılımı parametrelerinin tahmin edilmesinde Minitab yazılımı kullanılarak karşılaştırması yapılacak olan tasarımların Weibull dağılım grafikleri oluşturulmuş ve en küçük kareler yöntemi kullanılarak parametreler hesaplanmıştır. Yapılan tüm değerlendirmelerde, yalnızca metal dışı safsızlıklardan kaynaklanan hatalar göz önünde bulundurulmuş ve diğer hatalar gözardı edilmiştir. Oluşturulan grafikler değerlendirilerek, dağılımın saha bilgilerinin isabetli şekilde temsil edip etmediği değerlendirilmiştir. Dağılımın saha verilerine uygunluğunun değerlendirilmesinde, korelasyon katsayısı ve saha verilerinin Weibull dağılımı grafiklerinde beklenen düz çizgi karakterinden sapma durumları dikkate alınmıştır. Gerekli durumlarda saha verisinin genel karakterinden sapma gösteren veriler gözardı edilmiş ve saha koşullarında hatanın kesinlikle görülmeyeceği bir sürenin var olma olasılığı gözetilerek sahada görülen hataların değerlendirmesi iki yerine üç parametrelili Weibull dağılımı ile tekrar edilmiş ve önceki değerlendirme ile karşılaştırılmıştır.

Sahada görülen hataların karakterinin anlaşılması ve değişik tasarımların sahada gözlemlenen güvenilirlik performansının karşılaştırılması için, bu tasarımların maruz kaldıkları yükler ve tasarım özellikleri göz önüne alınarak birer yük katsayısı hesaplanmıştır. Dağılım parametrelerinin karşılaştırılan enjektör memesi tasarımlarının değişik yük katsayıları ile değişme yönünde korelasyon gösterip göstermediği incelenmiştir.

Enjektör memelerinde gözlemlenen saha hata oranlarının çok düşük olması ve bu nedenle sahadan gelen hata sayısı ve bilgisinin azlığı nedeni ile, Weibull dağılım parametreleri yüksek bir isabetle hesaplanamamıştır. Bu nedenle yük katsayısı ve Weibull dağılım parametreleri arasında doğrudan bir korelasyon bulunamamıştır. Ancak, karşılaştırılan sahaların sahada gözlemlenen hata oranları yük katsayısına bağlı üstel bir korelasyon göstermiştir ve bu nedenle daha yüksek sayıda hatanın bilgisi kullanılarak hesap yapılması durumunda Weibull dağılımının, sahada metal dışı safsızlıkların neden olduğu hatalarının analizinde kullanılmasının uygun bir yöntem olma ihtimalinin olduğu sonucuna varılmıştır.

Weibull dağılımının sahadaki duruma ne derece uyumluluk gösterdiğini değişik bir yönden tekrar değerlendirmek amacı ile, daha önce saha bilgileri ayrı ayrı incelenen tasarımların toplamdaki genel karakteristiği analiz edilmiştir. Sonuçlar ve elde edilen Weibull dağılımı parametreleri ile farklı bir tasarımın saha bilgilerinden elde edilen sonuçlar ve Weibull dağılımı parametreleri karşılaştırılmıştır. Bu karşılaştırma sonucunda, sahada gözlemlenen hata oranlarının çok düşük olması ve bu nedenle sahadan gelen hata sayısı ve bilgisinin azlığı nedeni ile, Weibull dağılım parametreleri yüksek bir isabetle hesaplanamamıştır ve bu nedenle farklı bir tasarımın parametrelerinin doğrudan tahmin edilmesi mümkün olmamıştır. Ancak, daha önceki değerlendirmelerde kullanılan tasarımların genel karakteristiğini ifade eden şekil parametresi ile kontrol amacı ile kullanılan tasarımın saha karakteristiğini ifade eden

şekil parametresine yakın olduğu görülmüştür. Bu sonuç Weibull dağılımının, sahada gözlemlenen metal dışı safsızlıkların neden olduğu hatalarının analizinde kullanılmasının, daha yüksek sayıda hatanın bilgisi kullanılarak hesap yapılması durumunda uygun bir yöntem olması ihtimalini güçlendirmektedir.



1. INTRODUCTION

Looking back at the history of mobility, one can surely state that combustion has been a core process, catapulting mankind from riding animals to machine based transportation. The development of combustion engines and the advantages thereby obtained have boosted further research since the first uses of the kind of machine transforming chemical energy to kinetic energy through external or internal combustion.

As the industry grew into its size today, the CO_2 concentration of the Earth, which showed an increasing trend since the industrial revolution took pace (see Figure 1.1).

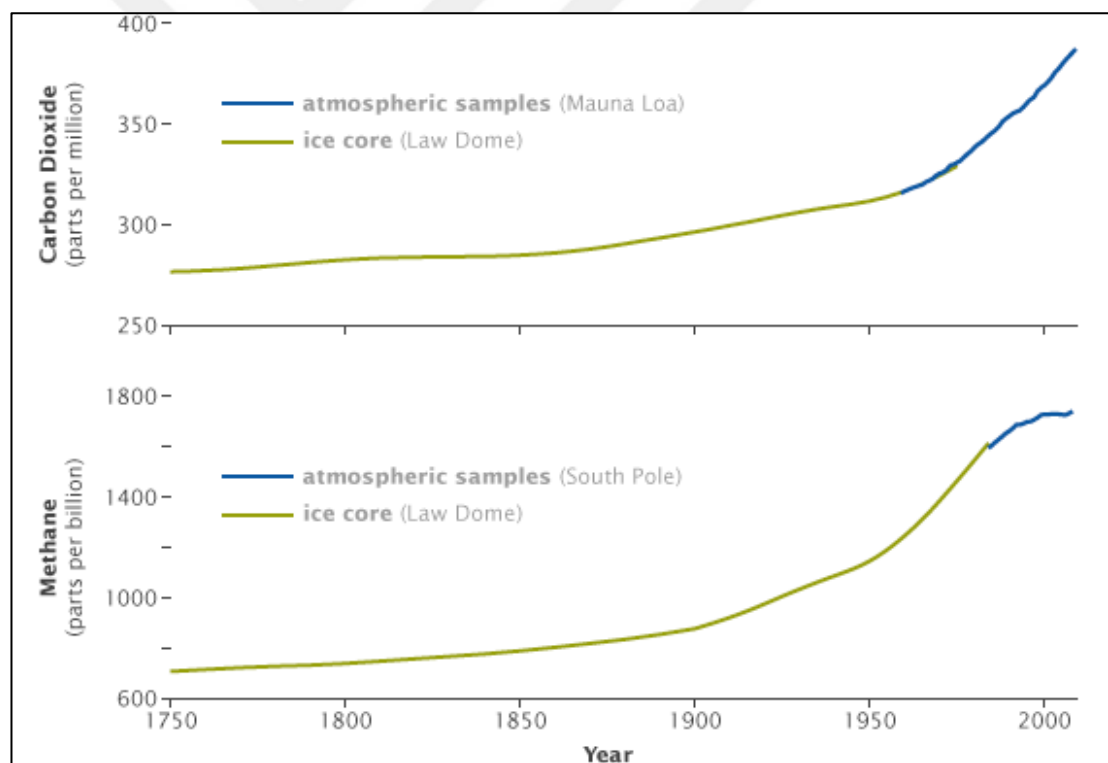


Figure 1.1: Change of carbon dioxide and methane with respect to years [Url-1].

Due to the increase of the CO_2 concentration, the greenhouse effect have become prominent, pushing the atmospheric temperature measurements higher and higher (see Figure 1.2).

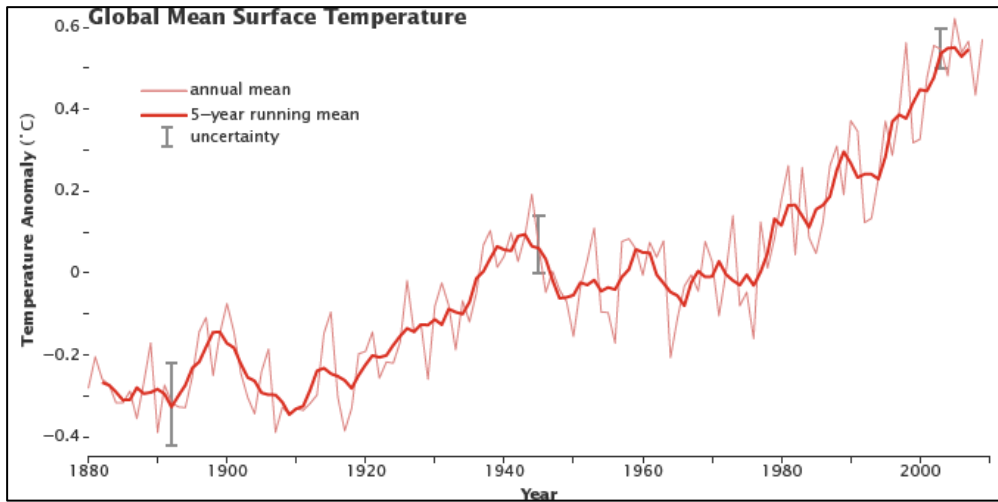


Figure 1.2: Change of calculated temperature anomaly with respect to years [Url-1].

Another problem which emerged with the wide use of internal combustion engines in vehicles is the ambient air quality going reduced by pollutants resulting from the chemical reactions taking place in the combustion process. Recent studies have shown that due to the relevant decrease of air quality through particulate matter, a vast number of people died in 2014 prematurely and that the the situation is expected to get better or worse in 2030 based on the application of further measures to decrease driving emissions (see Figure 1.3).

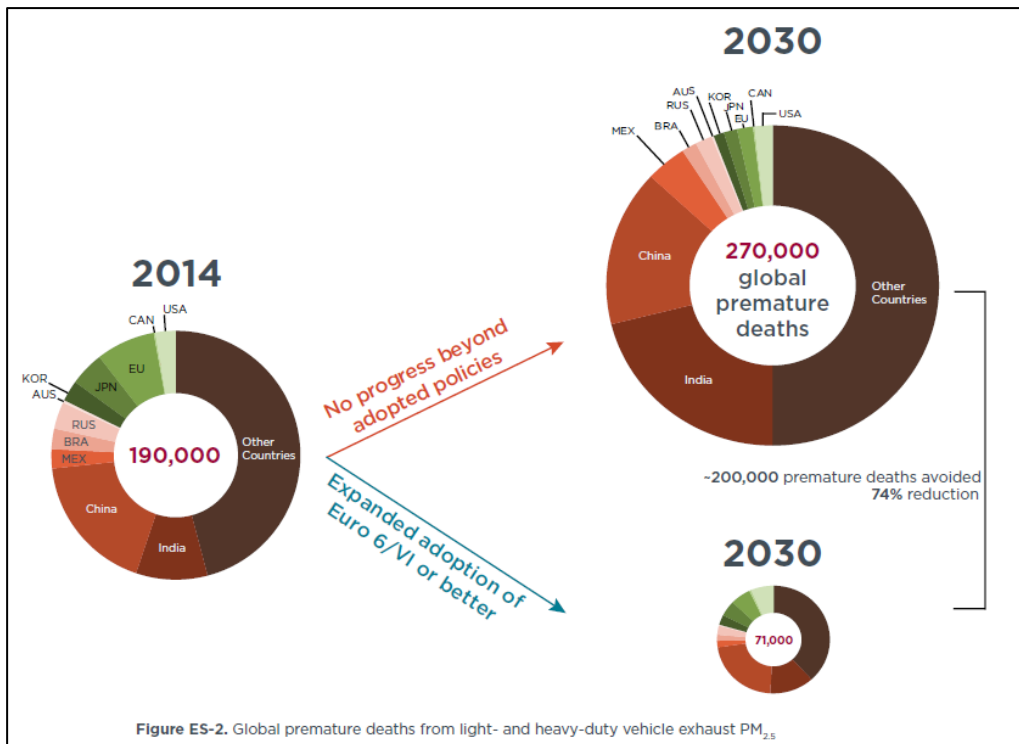


Figure 1.3: Global premature deaths from light and heavy duty vehicle exhaust PM (Miller et al, 2014).

In many cities, the WHO standards for air quality cannot be met. The scatter of PM with a diameter of 2,5 microns or less in the world can be seen below (see Figure 1.4).

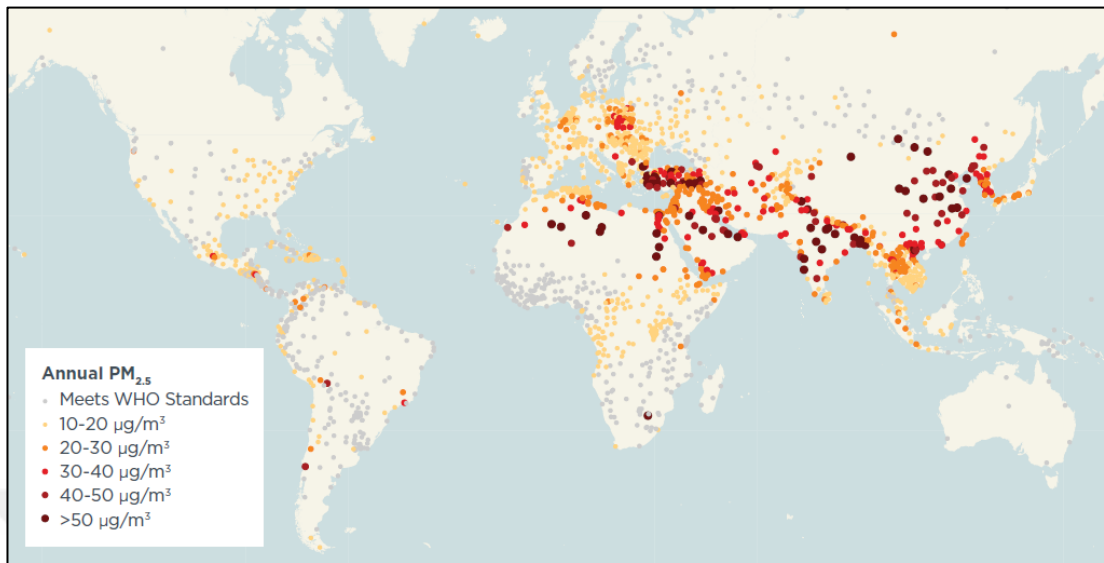


Figure 1.4: Worldwide PM 2.5 emission measurement results (Miller et al, 2014).

With ever bigger natural problems caused due to the increasing atmospheric temperature, measures were taken in order to limit and decrease the environmental damage. With the effect of emerging emission standards and times of crisis pushing the fuel prices higher, the manufacturers are forced to develop vehicles which are more economical and environmentally friendly, in order to keep up with the competitors and to comply with the laws.

Due to the increasing costs, and need for vehicles along with stringent emission standards, the claim for delivering “the best” has become even more vital for companies, pushing the engine and vehicle development targets in the direction of developing the best components and systems with minimum cost (see Figure 1.5). With car companies pushing the design limits further and further, contradicting design parameters make the development process more complicated and critical. For better fuel economy, performance and compliance with emission standards, the materials used for internal engines face increasingly higher loads, increasing the demand for lighter and stronger materials which can offer better resistance to demanding field conditions. With ever increasing loads on materials, the field observation becomes even more important.

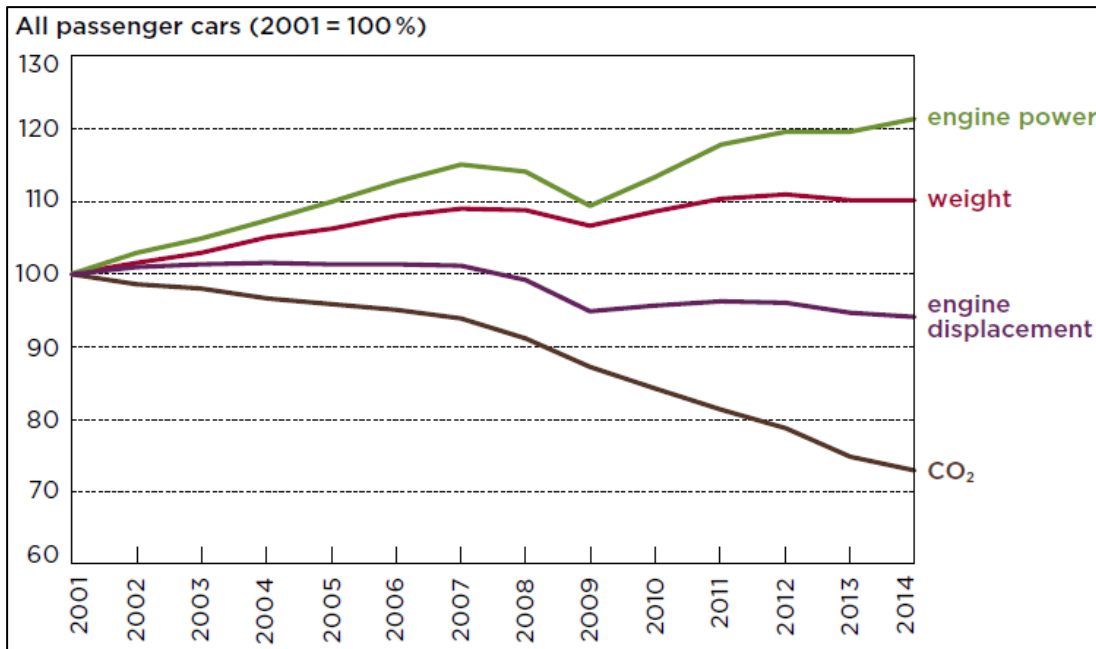


Figure 1.5: Change of vehicle technical parameters with respect to years (International Council on Clean Transportation, 2015).

The longing for faster, cheaper, more reliable and safer transport have created an industry in which competition has become inevitable. A wide diversity of choices and methods to design an internal combustion powertrain has become more and more standardized, as the legal requirements and customer expectations has eliminated all but the best combustion and emission control technologies.

One of the most important contributors in controlling diesel vehicle emissions have proven to be controlling the combustion process itself, using a highly versatile and precise fuel injection system. As the interface of the injection system to the combustion, the injector nozzles have developed in many aspects, enabling better fuel pulverisation and optimized use of the air inside the cylinders.

Diesel injector nozzles are expected to satisfy very low failure probability values in field when working under loads and conditions such as combustion and compression (engine brake) heat, corrosive combustion gases, combustion residues called “coking” and internal loads such as very high fuel pressure levels of up to 2500bar.

With design and manufacturing improvements enabling the nozzle manufacturing to meet higher and higher field loads, material defects such as non metallic inclusions gain importance, as they become the main cause for concern. The observation of the failure characteristics and statistics of a product in field can give the manufacturer an

overview of what the problem is, how the failure probability in field will change under which loads and design parameters. In the design phase of the product, it is necessary to estimate the risk due to material failures as well as validating the design, as the development tests can be done with limited number of samples, whereas a large quantity of a product is released after the design process for field operation. The evaluation and prohibition of field problems in the design phase of the product helps to minimize the costs through the lifetime, satisfy the customer quality expectations and maximize the profit.

A question raised during the design phase of diesel injector nozzles is whether it could be possible to estimate the field failure probability of diesel injector nozzles based on the field experience with the predecessors. It is aimed in this study, to search for a method to estimate the failure probability due to non metallic inclusions in steel.



2. DIESEL FUEL INJECTION SYSTEM

2.1 The Evolution of the Diesel Fuel Injection System

Diesel engines have gone through many stages of development until reaching the current widely utilized state of the art (see Figure 2.1). In the early industrialization phase, the diesel engine was mainly used as a replacement for bigger and less efficient steam engines, and on platforms which could accommodate large engines, such as ships, submarines, generators, locomotives and trucks. The use of a diesel engine in a car would not be seen until the debut of the Mercedes-Benz 260D in 1936, with 10 to 11 liters of fuel consumption per 100 kilometers at a time the price of diesel fuel was roughly half of of gasoline fuel (Wintrich et al, 2017).

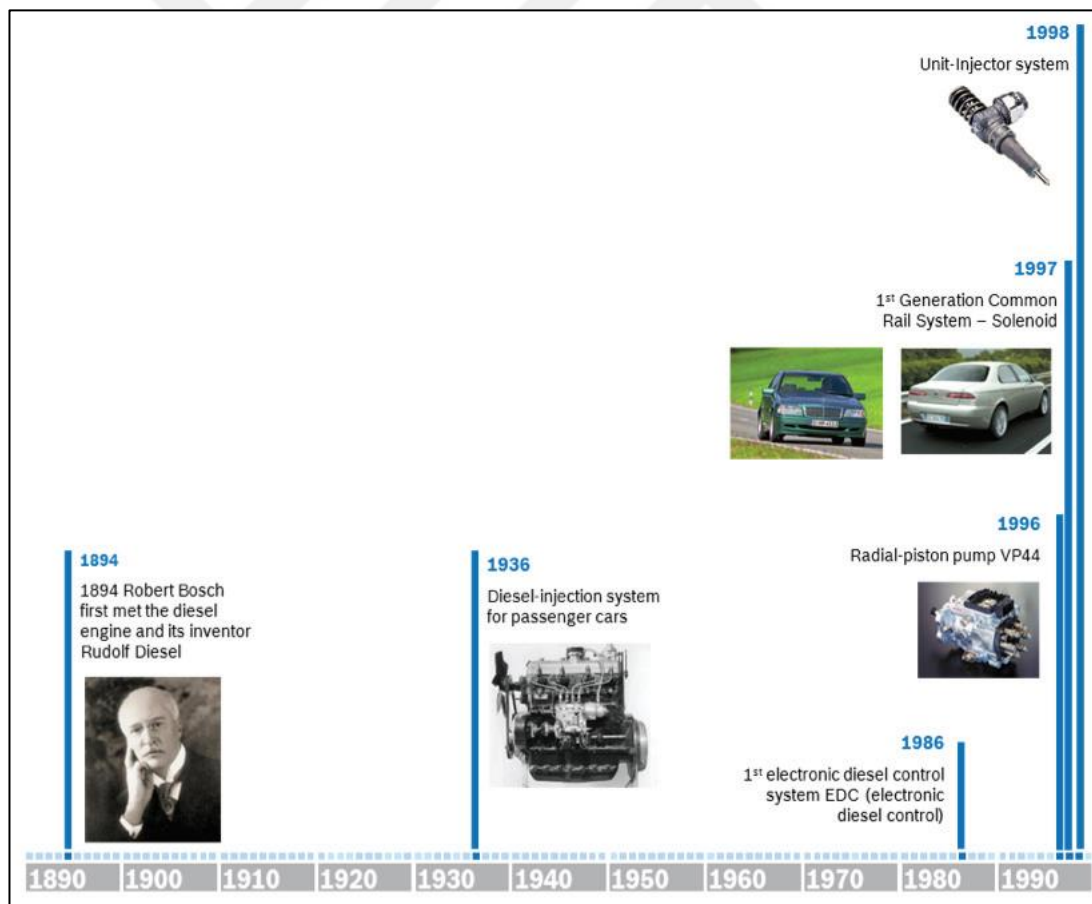


Figure 2.1: Diesel fuel injection system development milestones (Wintrich et al, 2017).

The start of manufacturing for diesel injection components gained pace with the first diesel pump prototypes in 1923, followed by the testing and approval of first samples by original equipment manufacturers and then the start of series manufacturing in 1936 (Wintrich et al, 2017).

Further evolutions could be summarized below as:

- In 1986, diesel engines started to be governed by electronic circuits, significantly improving the precision of fuel metering.
- In 1989, a diesel injection system used in the Audi 100TDI with an electronically governed high pressure pump, 950 bar injection pressure, a multi-sprayhole nozzle, turbocharger and pilot injection capability made way for the wide use of diesel engine in cars.
- In 1996, the injection pressure rose to 1800bar and the injection quantity had become precise down to the level of 2 mm^3 diesel fuel for pilot injection.
- In 1998, the unit injector system with 2050 bar injection pressure was introduced.
- In 1997, the first common-rail system with 1350 bar injection pressure was introduced, enabling the independence of injection timing, injection pressure from engine load and speed conditions.
- In 2003, the second generation common-rail system with 1600 bar injection pressure was introduced. This generation had better precision for smaller pilot injection amounts and smaller hydraulic dwell times between each injection.
- In 2003, the third generation common-rail system with 1600 bar injection pressure was introduced as well. This generation had higher precision based on a piezo actuator, thereby improving raw engine emissions through capabilities such as enhanced multiple injection performance and the ability to reach higher injection rates faster.

After the introduction of the second and third generation common rail injectors, the injection pressure was constantly improved up to 2500 bar (Wintrich et al, 2017).

2.2 The Diesel Injector Nozzle

The diesel injector nozzle is the most critical and important part of the whole injection system with many functions and targets related to engine objectives, as it is the interface of the fuel injection system to the combustion chamber and cylinder (see Figure 2.2). The function of the rest of the system, including the injector is to deliver the needed fuel quantity to the nozzle, to lift the needle at the start of the injection and to close it at the end of injection.

The main functions of the nozzle can be summarized as:

- The create and regulate the injection pressure and volume with respect to crankshaft angle.
- Optimum atomization and distribution of fuel
- To seal the whole injection system against the combustion conditions (Reif, 2012).

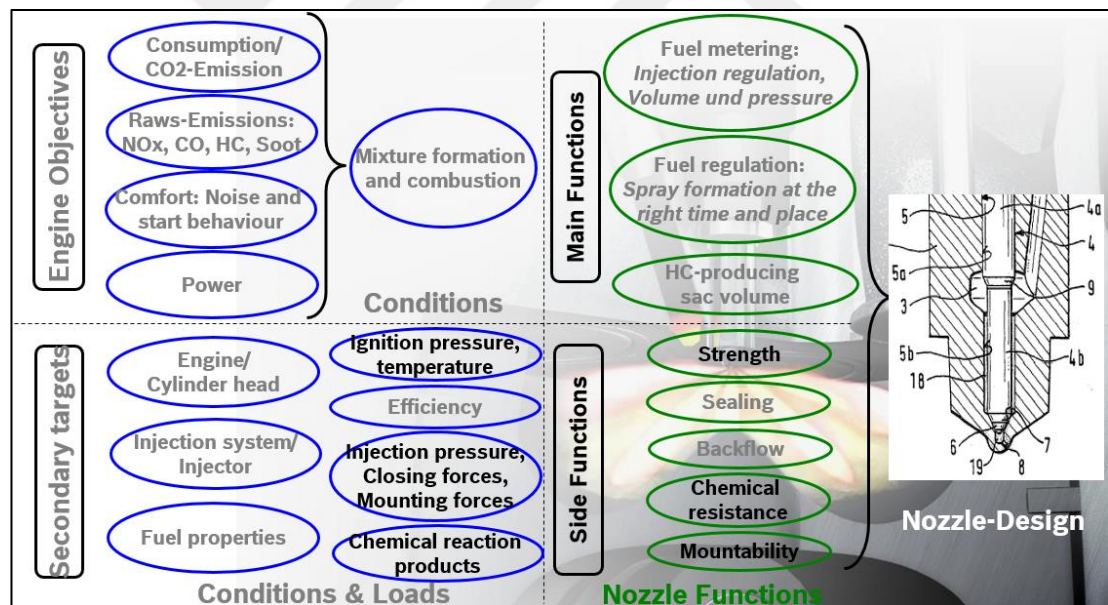


Figure 2.2: Objectives and functions related to the diesel injector nozzle (Robert Bosch GmbH, 2015).

The nozzle design has many major effects on the characteristics of the engine such as cold startability, power and emission output. It directly interacts with the cylinder, injector and the fuel itself. Therefore a diesel injector nozzle design is made focusing on the aimed engine characteristics and with mechanical and chemical durability mind.

The mechanical loads on diesel injector nozzles have increased tangibly with the need of higher injection pressure in order to enable lower emissions.

The effect of higher injection pressure on emissions and the load on the nozzles can be shown with the following chain:

- NO_x limits have been getting more and more stringent as stricter emission standards have emerged.
- Higher EGR usage is needed in order to keep NO_x emission under control and within the limits dictated by the emission standards.
- The air inside the cylinders is diluted more as more EGR gas is used to lower the combustion temperature.
- Lower oxygen content is available due to air dilution inside the cylinders.
- Higher PM emission is produced due to the lower oxygen content, as the available oxygen content is insufficient to efficiently oxidize the carbon atoms inside the fuel.
- Better air-fuel mixture is needed in order to improve the PM emission output.
- Lower sprayhole diameter is needed in order to deliver better air-fuel mixture.
- Higher injection pressure is needed to deliver the needed injection quantity within the specified crank angle period, despite higher flow restriction due to smaller sprayholes.
- Higher pressure is needed inside the nozzles and the common rail system in order to deliver higher injection pressure.
- Higher internal pressure inside the nozzles cause higher load on the injector nozzles

With the need to implement higher injection pressure, higher accuracy and efficiency for fuel injection, the injector nozzles have evolved to the current state of the art (see Figure 2.3 and Figure 2.4). Today, widely utilized state of art nozzle designs can be divided into two main categories:

- P-Nozzle
- Nozzle module

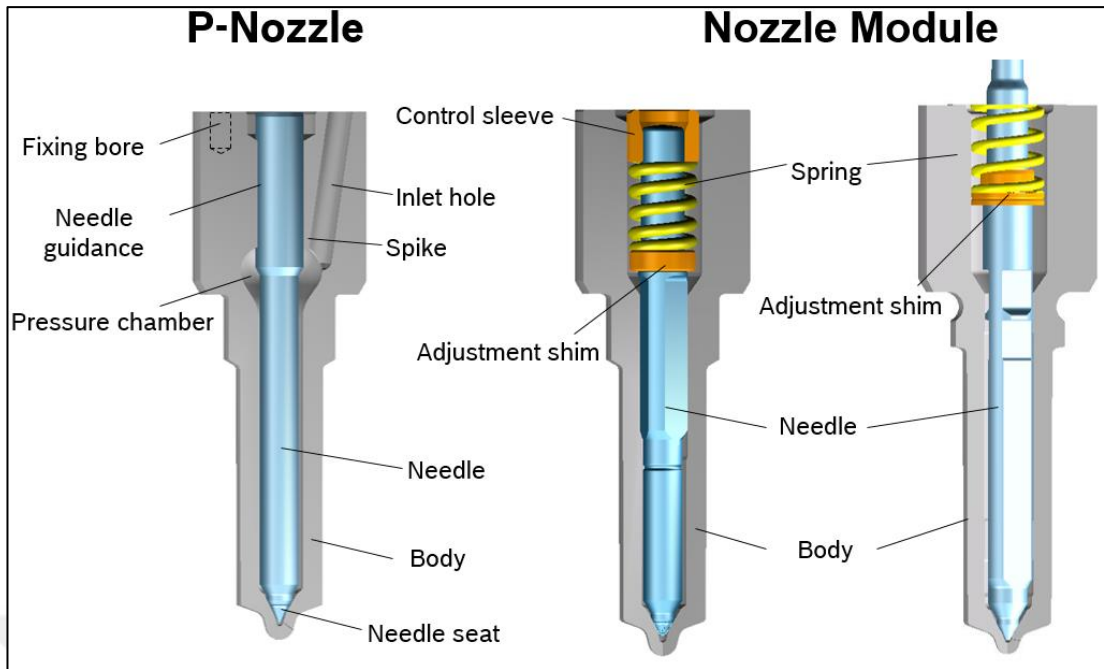


Figure 2.3: Modern diesel injector nozzle construction (Robert Bosch GmbH, 2015).

In both nozzle designs, there are specific regions which are highly loaded and therefore stressed. During the closing phase of the injector, the needle seat sits on the body seat and creates a sealing which stops the flow of the fuel into the cylinder. The closing forces during and after the closing phase of the injector are high in order to maintain the sealing function against the lifting force created by the high pressure acting on the needle.

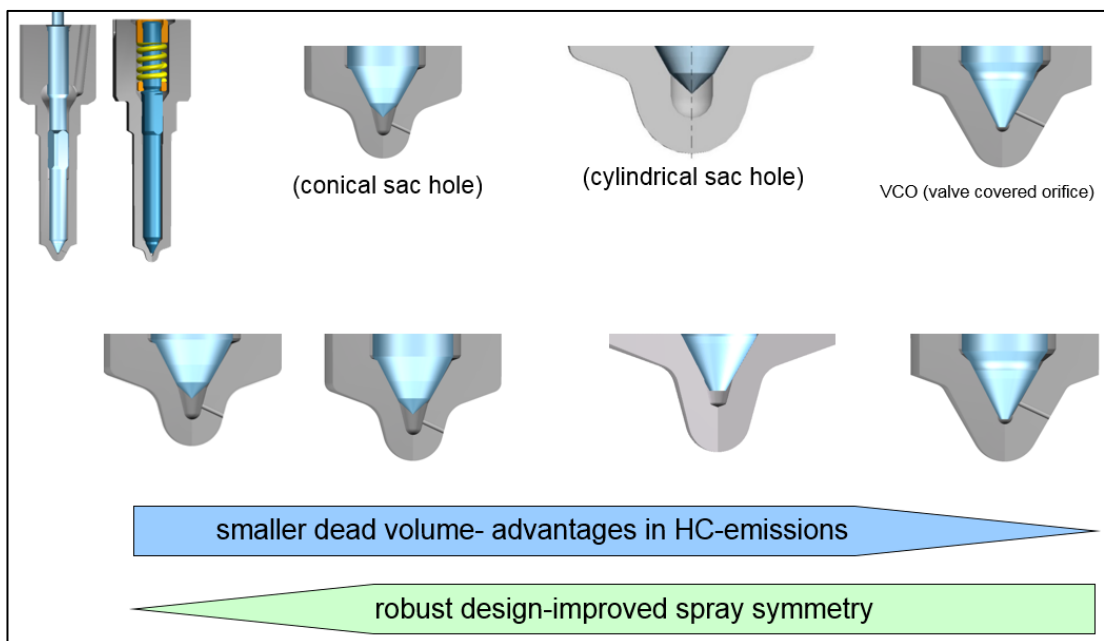


Figure 2.4: Sachole design and its effects on nozzle properties (Robert Bosch GmbH, 2015).

The design of the nozzle tip plays a major role both for the robustness and the emission performance of the nozzle. A bigger sacchole brings higher robustness and better spray symmetry due to smaller difference of fuel pressure at the entrance of the sprayholes, whereas a smaller sacchole brings smaller volume, in which the diesel fuel can reside between the injections. The heat from the cylinder promotes the evaporation of the fuel in this volume, thereby increasing the unburned HC emission of the vehicle.

The design is made with all effects in consideration and an optimum compromise is made based on the needs of the application.



3. IMPURITIES IN MATERIAL AND NOZZLE FAILURES

The robustness properties of the nozzle is equally dependant on the material and manufacturing. There are many aspects which should be satisfied by the nozzle material, including:

- Strength
 - High statistical strength
 - High strength againt pressure pulsation in the internal surfaces
 - High strength against the forces acting on the nozzle body seat under engine conditions such as high temperature
 - No flaws or irregularities are wanted
 - High material purity → Less quantity and smaller size of oxides and less number of sulfides
 - No brittle phases such as large carbides
- High wear resistance
- Good machinability properties
 - Adequacy for pressing operations
 - Temperability and hardenability
 - Adequacy for grinding and eroding operations
- Availability at large quantity and low cost (Robert Bosch GmbH, 2015).

During the casting sequence, melted steel inside the large melting pot is transferred via ladle and afterwards poured into the tundish. Inside the tundish, the flow of the steel is controlled by the stopper and the shroud and mold ensures that the casting is continuous. The steel is then transferred between rolls as it solidifies.

The required steel quality changes based on the product it will be used for and therefore the requirements related to the size, the amount and the composition of inhomogenities

inside the steel such as non-metallic inclusions also changes (see Table 3.1). An optimum compromise between quality and productivity is sought during the continuous casting of steel (Nakashima et al, 2013).

Table 3.1: Accepted adequate impurities and inclusion in steel products (Zhang et al, 2003).

Steel product	Maximum impurity fraction	Maximum inclusion size
Automotive & deep-drawing Sheet	[C]≤30ppm, [N]≤30ppm ¹³⁾	100μm ^{13, 14)}
Drawn and Ironed cans	[C]≤30ppm, [N]≤30ppm, T.O.≤20ppm ¹³⁾	20μm ¹³⁾
Line pipe	[S]≤30ppm ¹⁵⁾ , [N]≤35ppm, T.O.≤30ppm ¹⁶⁾ , [N]≤50ppm ¹⁷⁾	100μm ¹³⁾
Ball Bearings	T.O.≤10ppm ^{15, 18)}	15μm ^{16, 18)}
Tire cord	[H]≤2ppm, [N]≤40ppm, T.O.≤15ppm ¹⁶⁾	10μm ¹⁶⁾ 20μm ¹⁴⁾
Heavy plate steel	[H]≤2ppm, [N]30-40ppm, T.O.≤20ppm ¹⁶⁾	Single inclusion 13μm ¹³⁾ Cluster 200μm ¹³⁾
Wire	[N]≤60ppm, T.O.≤30ppm ¹⁶⁾	20μm ¹⁶⁾

During continuous casting, inhomogenities such as non-metallic inclusions can occur due to a number of reasons and at certain steps of the process (see Figure 3.1). With respect to the source they originate from, inclusions can be classified as:

- Indigenous Inclusions
 - Deoxidation products
 - Precipitated inclusions which are created during cooling and solidification steps
- Exogenous Inclusions
 - Reoxidation products
 - Slag entrainment products
 - Inclusions formed due to erosion/corrosion of refractory lining
 - Inclusions from chemical reactions (Zhang et al, 2003).

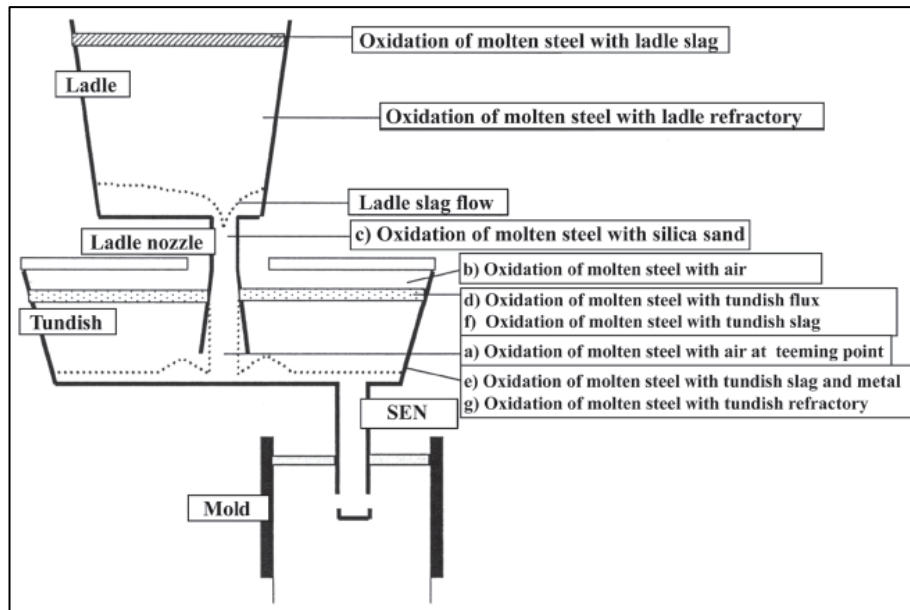


Figure 3.1: Diagram showing molten steel reoxidation (Nakashima et al, 2013).

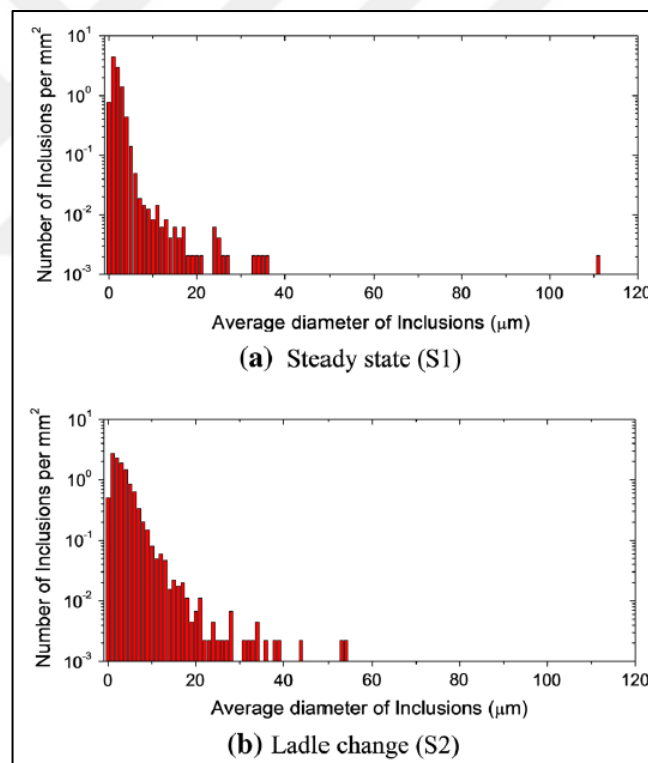


Figure 3.2: Size distribution of oxide inclusions during steady state casting and ladle change (Ren et al, 2014).

While the steel is being continuously cast, oxide inclusions form during the process steps in which the steel is in liquid state and sulfide inclusions precipitate during later process steps of cooling and solidification. As seen in Figure 3.2, the oxygen content

as well as the quantity of oxide and sulfide inclusions are increased during the ladle change period, compared to the steady state casting conditions (Ren et al, 2014).

Along with their direct effect on steel characteristics and quality, NMIs also have indirect effects such as clogging casting nozzles as seen in Figure 3.3, resulting in process problems such as molten steel drift in mold and powder entrapment (Nakashima et al, 2013).

While the steel is continuously transferred from the tundish to the mold, the inclusions can attach to the submerged entry nozzle installed to the tundish, in case the inclusions inside the molten steel are not in fluid form.



Figure 3.3: Clogging materials (mainly $Al_2O_3 - CaO - MgO$ inclusions) at the submerged entry nozzle (Ren et al, 2014).

This can cause severe clogging and in some cases, an interruption of the casting process as the steel can no longer flow through the nozzle. As shown in Figure 3.4, the inclusions disengaging from the nozzle is also an important reason for relatively big sized Al_2O_3 inclusions (Ren et al, 2014).

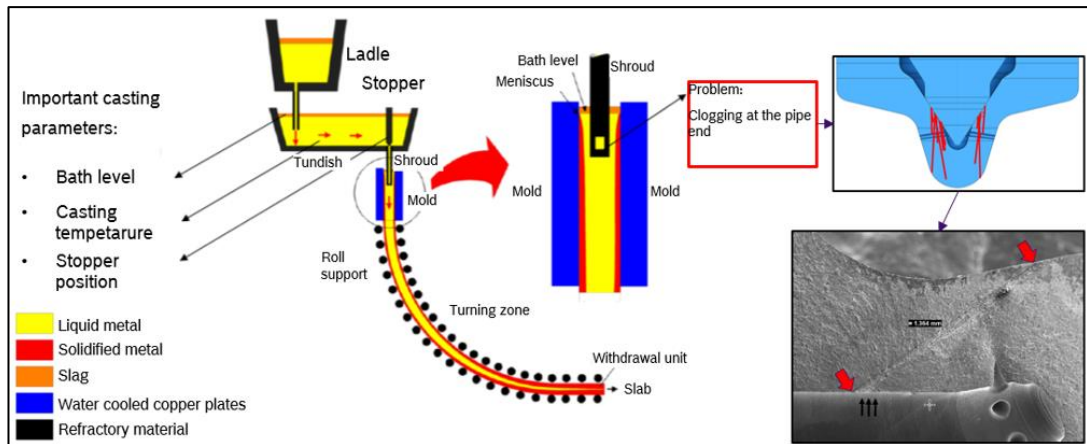


Figure 3.4: Formation of non-metallic inclusions (Robert Bosch GmbH, 2017).

The size of the inclusions is very critical as the deterioration of mechanical properties is significantly increased as the inclusion size increases (see Figure 3.5). Smaller inclusions can be found in higher quantities as larger inclusions are rarer. The total volume fraction can be higher either for smaller or bigger inclusions. The ductility and of the steel deteriorates in cases with higher oxide or sulfide content. Fracture toughness is also negatively effected for high strength steels (Zhang et al, 2003). As seen in Figure 3.6 and Figure 3.7, the oxygen content and the number of inclusions above a critical size can be decisive on the lifetime of the product.

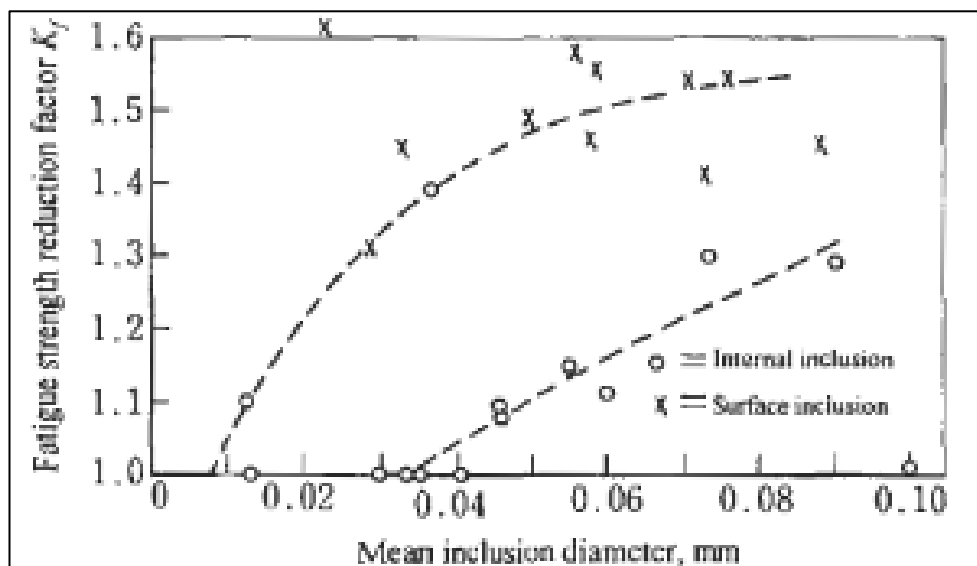


Figure 3.5: Fatigue strength reduction factor vs mean inclusion diameter (Murakami, 2002).

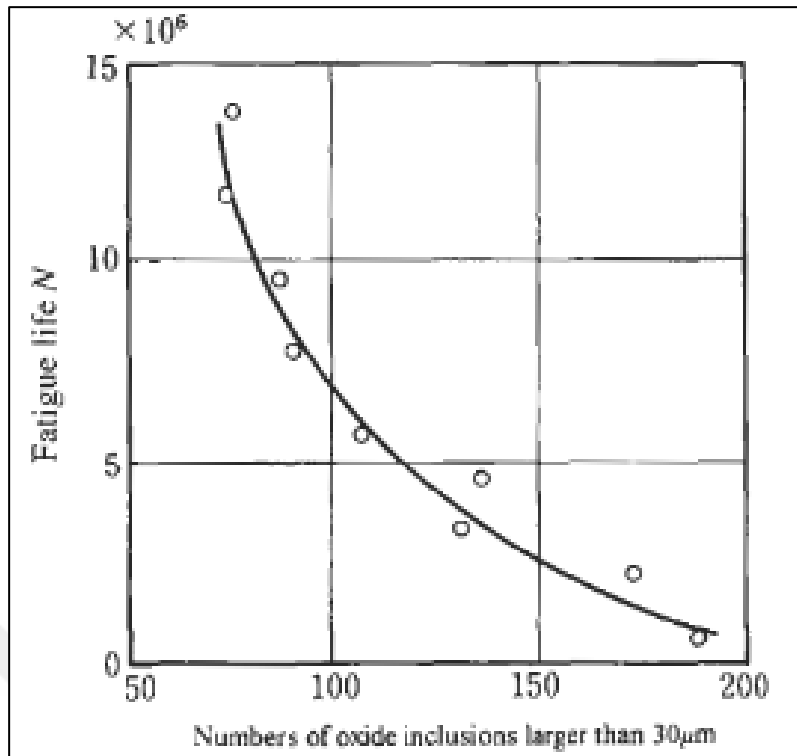


Figure 3.6: Flaking life of ball bearings vs the number of oxide inclusions (Murakami, 2002).

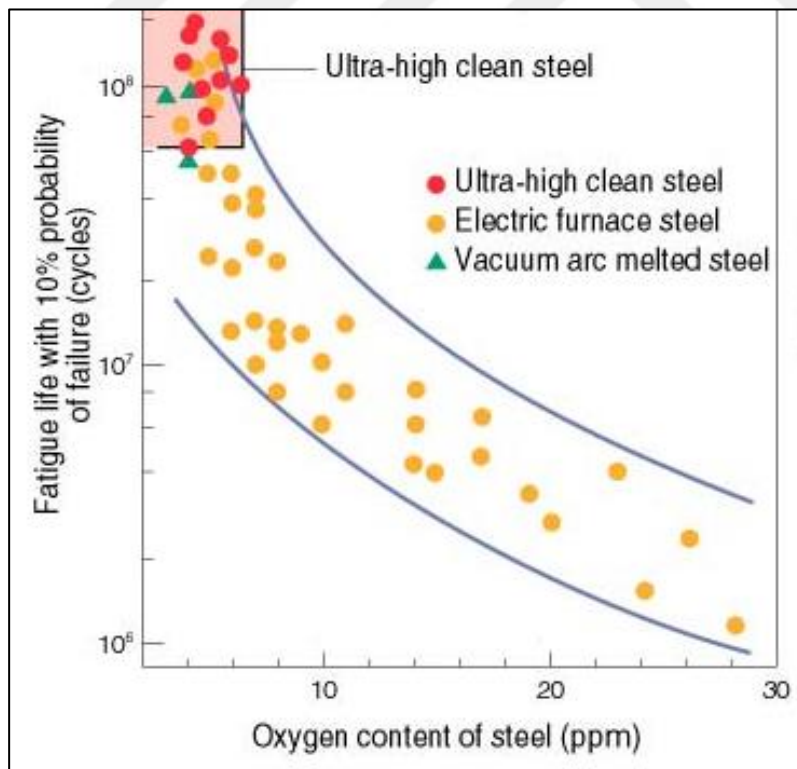


Figure 3.7: Fatigue life with 10% failure probability with respect to oxygen content of steel (Zhang et al, 2003).

The hardness of the inclusions after solidification of steel dictates whether the inclusion will deform along with the steel in the following deforming operations such as rolling (see Figure 3.8).

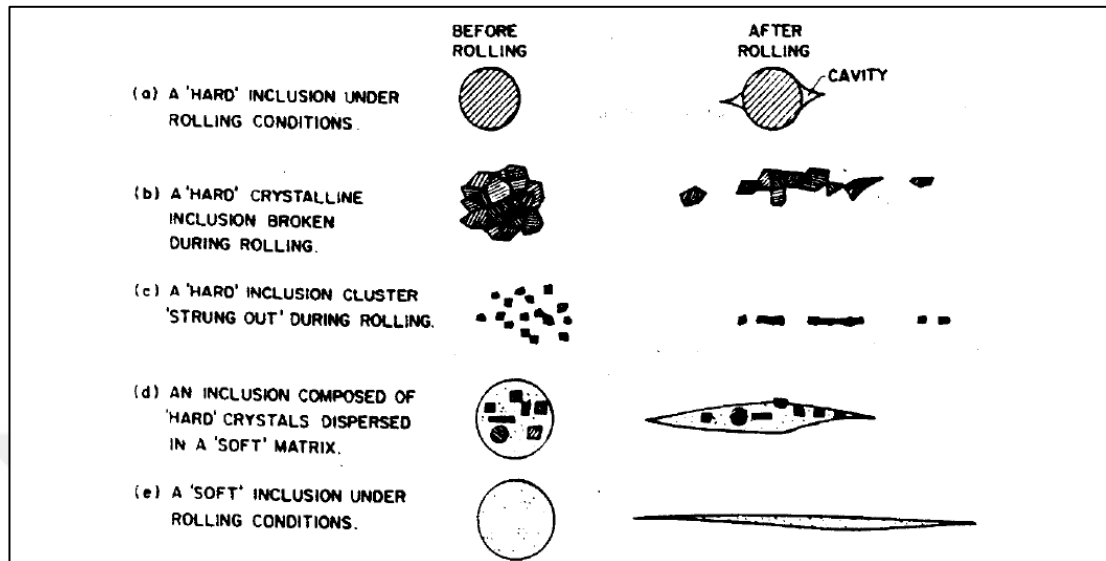


Figure 3.8: Inclusion forms of hard and soft inclusions before and after rolling (Zhang et al, 2003).

The inclusions, inhomogenites and other defects have the effect of influencing the crack initiation based on their shape and their size have a crucial effect on the fatigue limit. For steels with high hardness of more than 400HV, the fatigue strength reduction due to this effect can be greater than that of steel microstructure and hardness and therefore the size, quantity and the distribution of inclusions is often the point with the highest improvement potential for lower field failure probability (Murakami, 2002).

For the aim of detecting NMIs in end products, various methods can be utilized. Detection of NMIs by X-ray computed tomography makes it possible to detect NMIs without a destructive operation, but has the downsides of being time consuming besides other difficulties such as high absorption in steel, limited penetration lengths, image noise, and contrast problems caused by artifacts.

Fatigue life testing, an destructive test method can be used in order to measure and detect critical sized NMIs. After the testing for a failed sample is completed, the fracture surface can be analyzed using scanning electron microscope and energy dispersive X-ray spectroscopy can be utilized in order to identify the characteristics of the NMI in question (Gusenbauer et al, 2014).

Based on their size, non-metallic inclusions can be grouped in two main categories as microscopic and macroscopic inclusions. Inclusions allocating up to a maximum area of $0,03 \text{ mm}^2$ on the polished specimen surface are categorized as microscopioic inclusions, whereas larger inclusions are called macroscopic inclusions. At the stage of steel bar manufacturing, the microscopic degree of purity for the steel is evaluated with respect to either a maximum size rating values or an index indicating percentage of area for inclusions larger than a specified size, both for sulfuric and oxidic inclusions, using a metallurgical microscope and automated devices (Norm, D. I. N., 1985).

An inline ultrasound testing along with Eddy-current testing is utilized in order to find out whether the steel bars include macroscopic inclusions above a certain size.

4. WEIBULL ANALYSIS

The Weibull distribution is often preferred as a basis for lifetime analysis to model the field situation due to its versatility and its ability to give the researcher accurate predictions based on limited number of failures. With more failures involved in the analysis, the model suggested by the distribution gets more accurate.

For the field analysis of products, Weibull analysis is chosen as it is very often the preferred lifetime distribution to model field problems. Based on the shape parameter, the Weibull ditribution is also able to behave similarly to the other distributions. Unlike the exponential function, the Weibull function can model situations in field, where the failure probability changes with respect to time. The most common applications of Weibull analysis include the field performance evaluations of electron tubes, relays, ball bearings, as well as weather forecasts, wind speed estimations and signal level distributions of radar systems (Türkan, 2007).

The characteristics defining the shape of the Weibull curve are:

β : Shape parameter (also called slope)

η : Scale parameter (also called characteristic life)

γ : Location parameter (also called failure free life)

The Weibull probability density function can be written as:

$$f(t) = \frac{\beta}{\eta} \left(\frac{t-\gamma}{\eta} \right)^{\beta-1} e^{-\left(\frac{t-\gamma}{\eta} \right)^\beta} \quad (4.1)$$

$$f(t) \geq 0, t \geq 0 \text{ or } \gamma$$

$$\beta > 0$$

$$\eta > 0$$

$$-\infty < \eta < \infty$$

In case the location parameter γ is 0 or in other words when the failures can be observed immediately after the product is introduced to the field, the Weibull probability density function can be written in the 2-parameter form:

$$f(t) = \frac{\beta}{\eta} \left(\frac{t}{\eta}\right)^{\beta-1} e^{-\left(\frac{t}{\eta}\right)^\beta} \quad (4.2)$$

In special cases where the shape parameter β is also already known from previous similar products, the probability density function can be written in the 1-parameter form:

$$f(t) = \frac{c}{\eta} \left(\frac{t}{\eta}\right)^{c-1} e^{-\left(\frac{t}{\eta}\right)^c} \quad (4.3)$$

$$\gamma = 0$$

$$\beta = c = \text{Constant}$$

As seen in Figure 4.1, with respect to the value of the shape parameter β , the function can display a character similar to other lifetime distributions. In a situation where the shape parameter β is equal to 1, the Weibull PDF becomes a 2-parameter exponential distribution function:

$$f(t) = \frac{1}{\eta} \exp\left(-\frac{t}{\eta}\right) \quad (4.4)$$

where $\frac{1}{\eta}$ = failure rate

In another situation where the shape parameter β is equal to 2, the Weibull probability density function then becomes the same as that of the Rayleigh distribution. The shape parameter is dimensionless (Çakır, 2009).

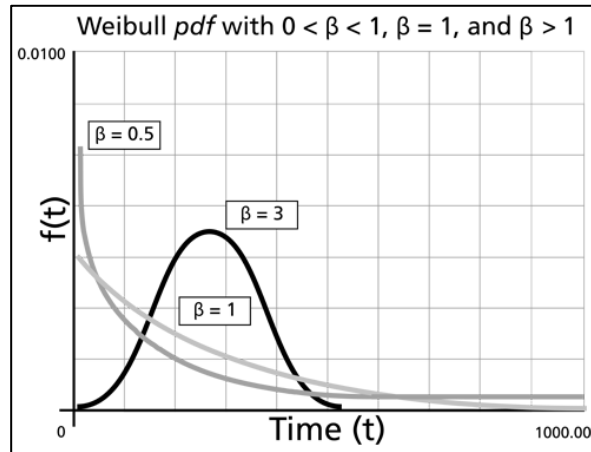


Figure 4.1: Weibull probability density function with respect to β value [Url-3].

On the cumulative distribution function graph, the slope of the line representing the field failures change with respect to the shape parameter β (see Figure 4.2).

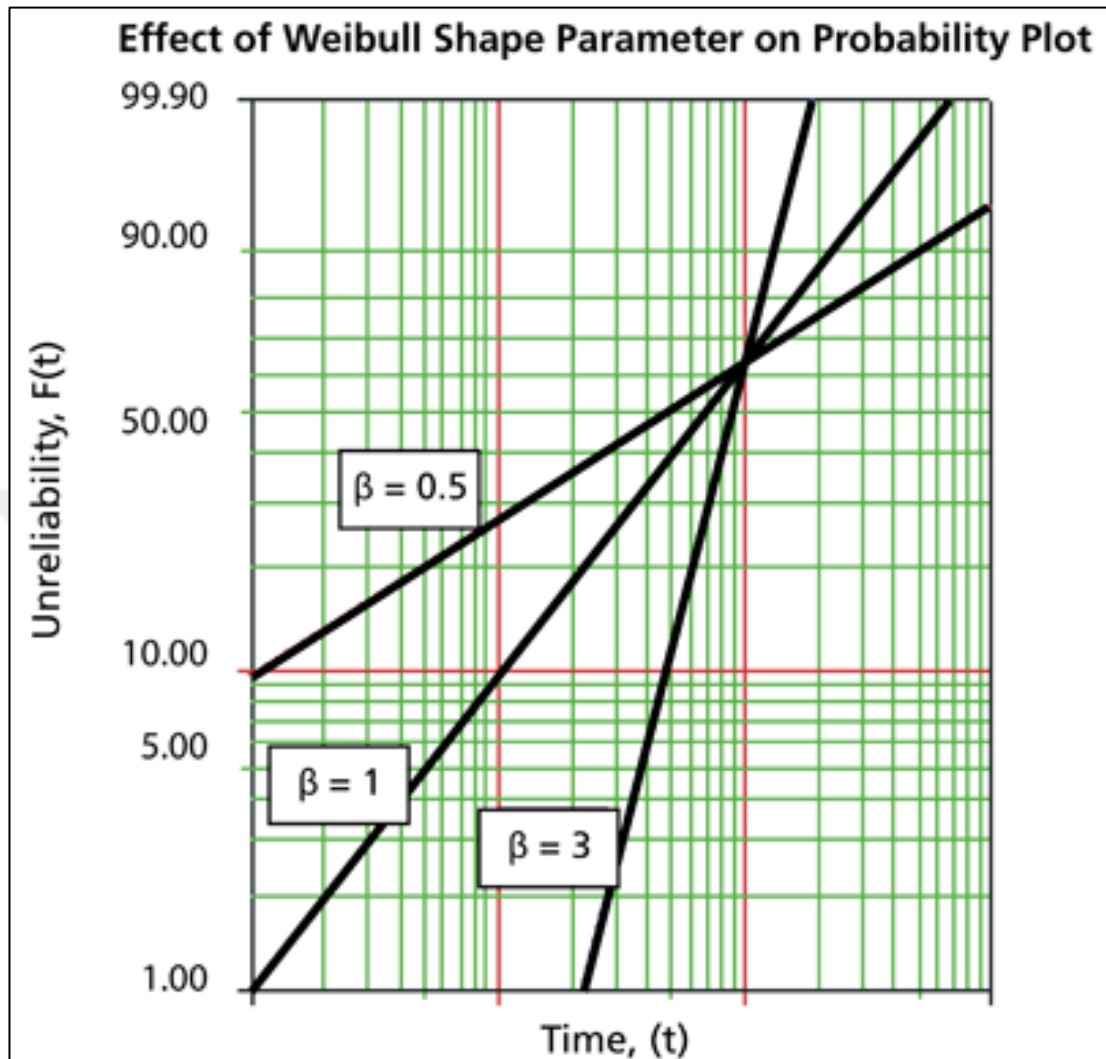


Figure 4.2: Effect of shape parameter β on unreliability [Url-3].

As shown in Figure 4.3 and Figure 4.4, the value of the shape parameter dictates how the reliability and failure rate changes over the lifetime. For different values of the shape parameter, the following comments can be made:

$\beta < 1 \rightarrow$ Infant mortality, decreasing failure rate over lifetime

$\beta = 1 \rightarrow$ Random failures, constant failure rate over lifetime

$\beta = 3 \rightarrow$ Early wearout, increasing failure rate over lifetime

$\beta = 6 \rightarrow$ Old age wearout, increasing failure rate over lifetime (Abernethy et al, 1983)

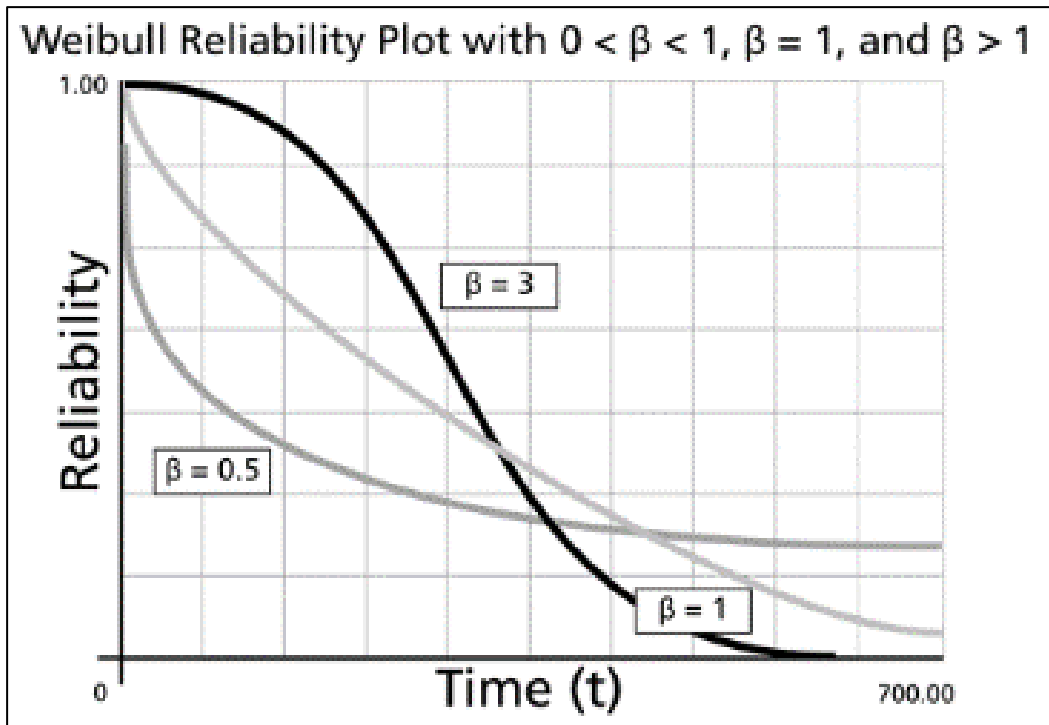


Figure 4.3: Effect of shape parameter β on reliability [Url-3].

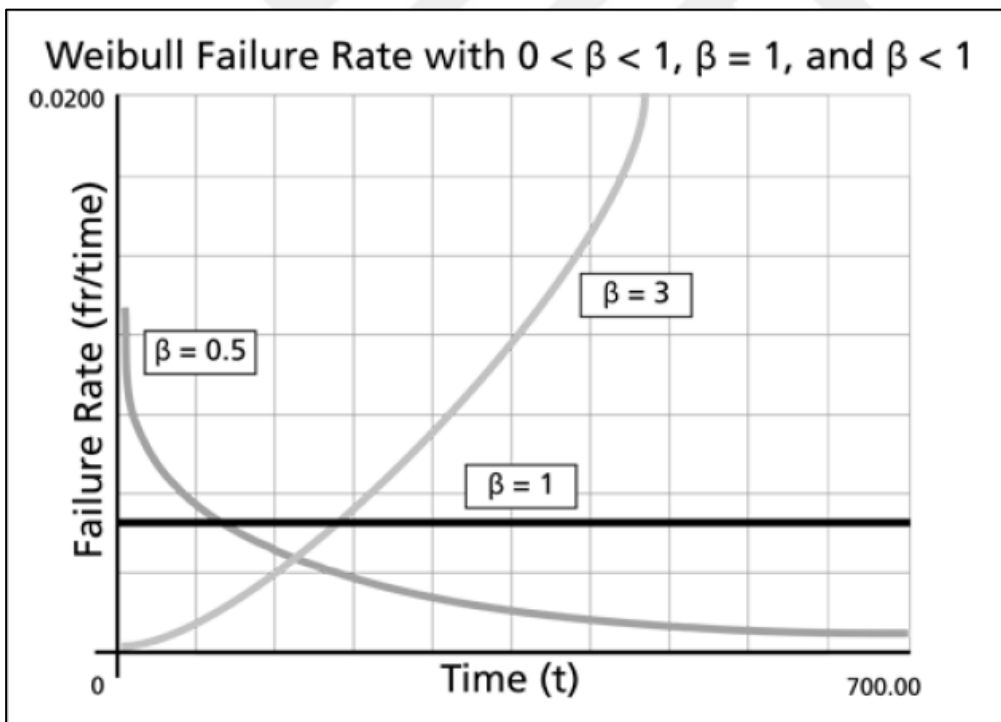


Figure 4.4: Effect of shape parameter β on failure rate [Url-3].

The scale parameter η is the interval at which 63,2 percent of the failed parts complete their lifespan (see Figure 4.5). Therefore as the shape parameter gets higher, the Weibull plot is shifted to the right, the probability density function gets wider towards higher time or mileage (see Figure 4.6).

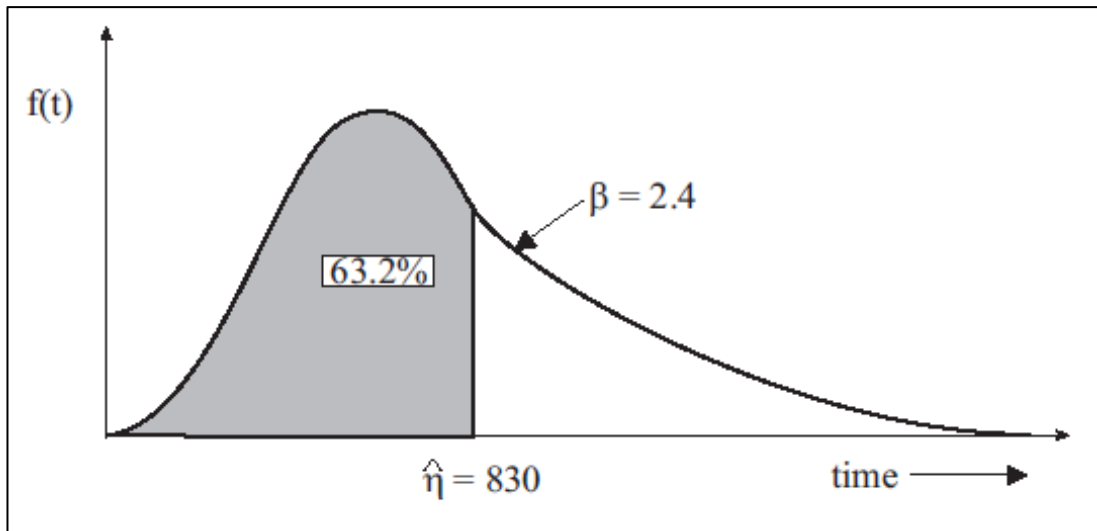


Figure 4.5: Weibull PDF and characteristic life (Warwick Manufacturing Group, 2004).

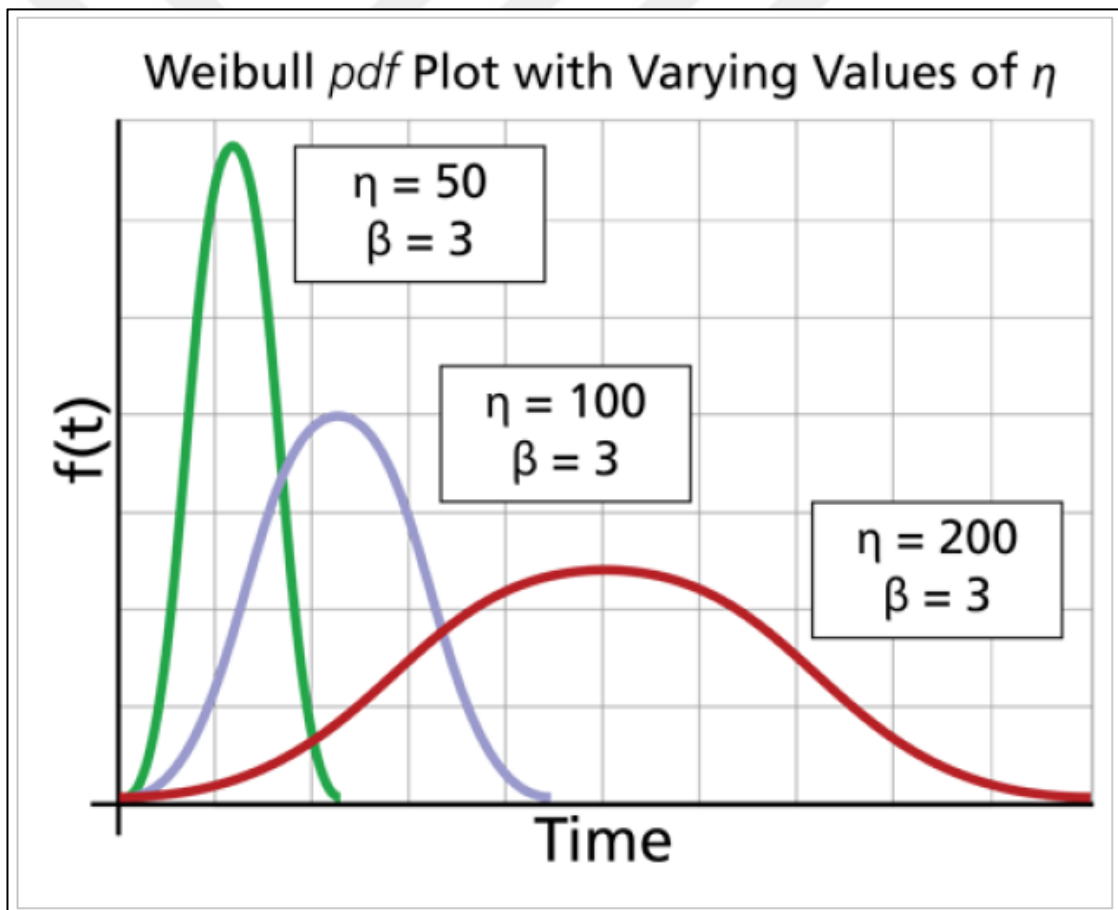


Figure 4.6: Weibull PDF and scale parameter η [Url-3].

As seen in Figure 4.7, the location parameter γ shifts the whole probability density function and therefore the Weibull unreliability plot towards higher time period or

maileage before failure. It defines a time interval, before which any failure in field can not happen.

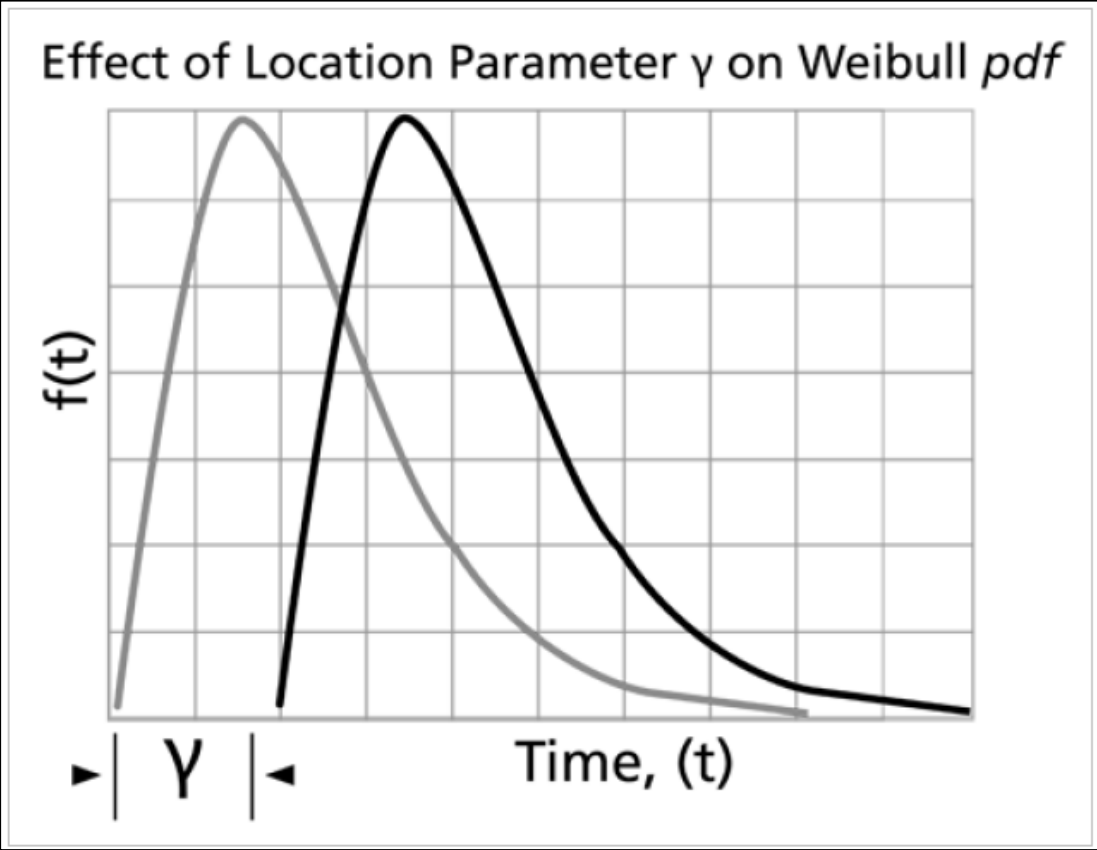


Figure 4.7: Weibull PDF and location parameter γ [Url-3].

5. EVALUATION OF NON METALLIC INCLUSION RELATED NOZZLE FIELD FAILURE PROBABILITY

In order to satisfy the needs of the automotive industry, millions of injector nozzles are sent to field annually. Due to a variety of reasons, a certain quantity of nozzles fail to reach their lifetime goal. The leading reasons for diesel injector nozzle failures are:

- Non metallic inclusions inside the steel
- Hydrogen stress corrosion cracking
- Thermal overload

When we try to focus on the root cause with the highest priority, the overview of the field records show that around 80% of the nozzle failures in field are caused by non-metallic inclusions (NMIs), which are the byproduct of the steelmaking process, effecting the cleanliness of the steel in a negative way (see Figure 5.1).

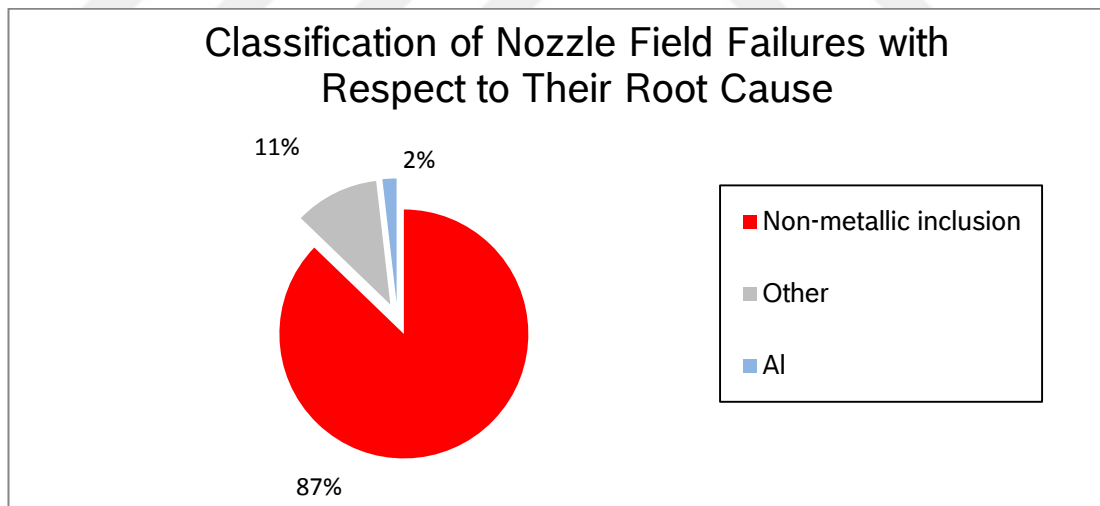


Figure 5.1: Classification of nozzle failures with respect to their root cause (Robert Bosch GmbH, 2017).

During the manufacturing processes of the nozzle, these non metallic inclusions can be cut. Whereas the presence of non metallic inclusions are never welcome, their presence in the nozzle body seat area is more critical as the seat area is subjected to impact forces during the closing phase of the injector, and the angular shape of the

nozzle body seat increases the risk of exposing the NMI to the surface during manufacturing operations.

NMIs causing nozzle tip cracks are observed in different shape and sizes. Examples for main inclusion shapes observed on parts which cracked in field are given in the following pages, starting with Figure 5.2 and ending with Figure 5.9.

Globe Shaped Inclusions (see Figure 5.2 and Figure 5.3):

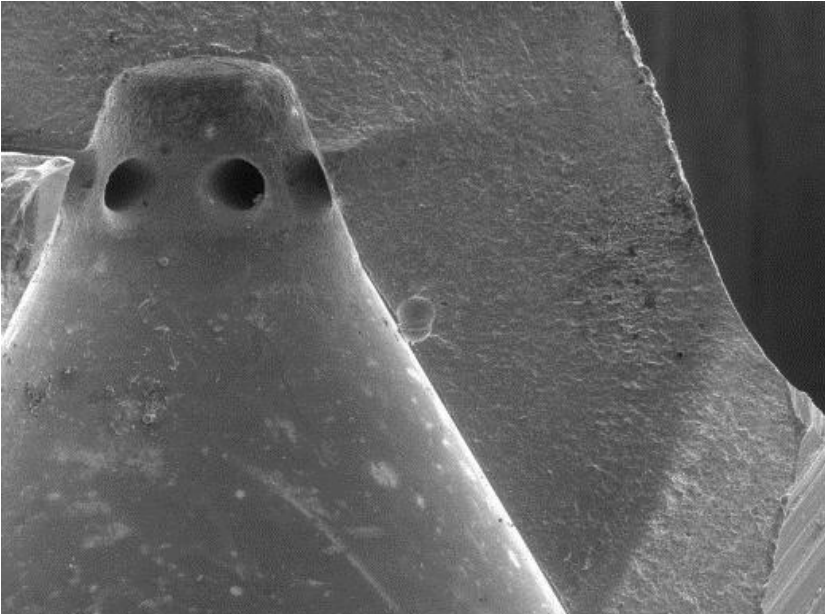


Figure 5.2: SEM photograph of a diesel injector nozzle (Robert Bosch GmbH, 2014).

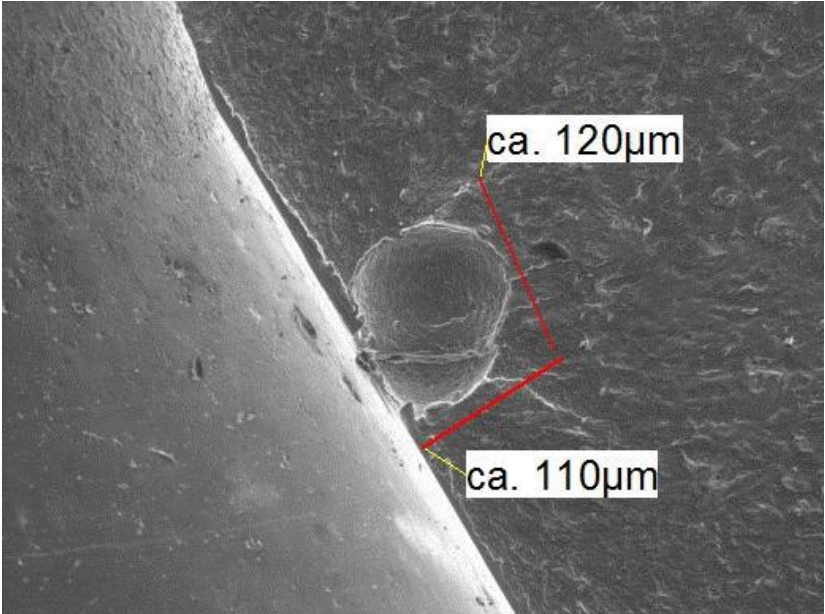


Figure 5.3: SEM photograph of a diesel injector nozzle (Robert Bosch GmbH, 2014).

Line Shaped Inclusions (see Figure 5.4 and Figure 5.5):

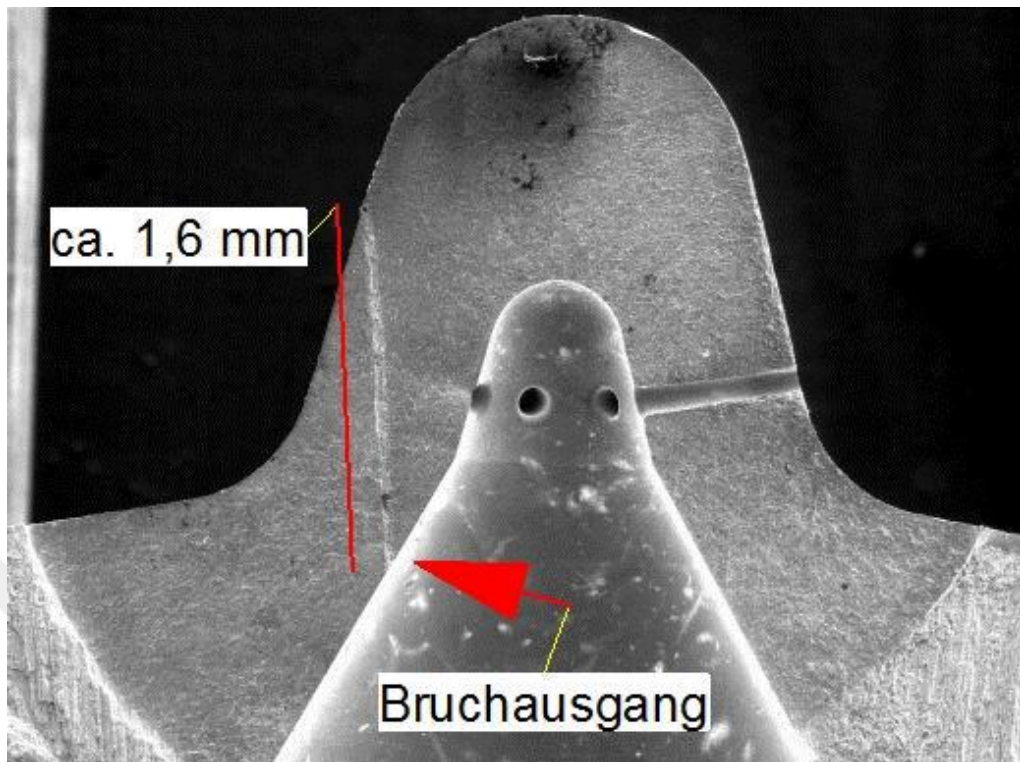


Figure 5.4: SEM photograph of a diesel injector nozzle (Robert Bosch GmbH, 2014).

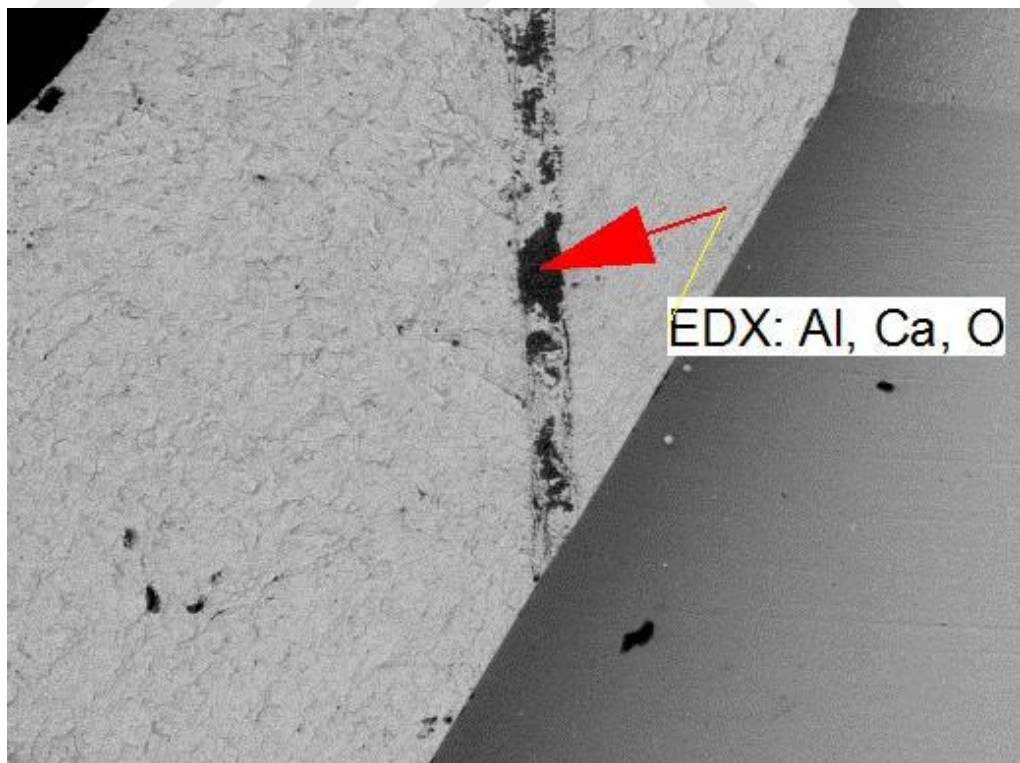


Figure 5.5: SEM photograph of a diesel injector nozzle (Robert Bosch GmbH, 2014).

Cigar Shaped Inclusions (see Figure 5.6, Figure 5.7, Figure 5.8 and Figure 5.9):

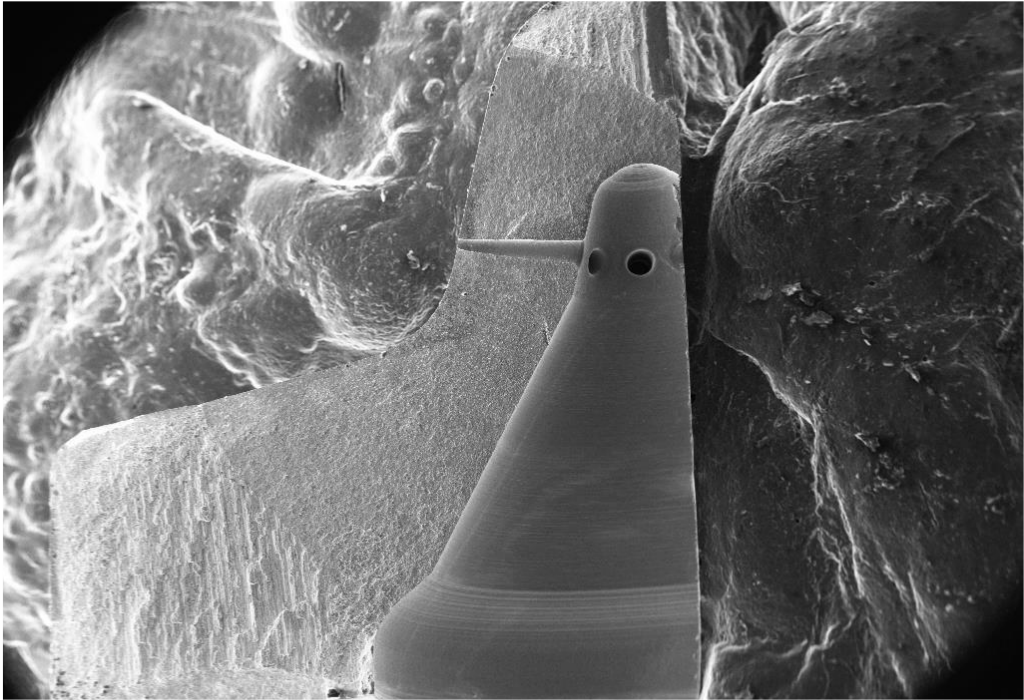


Figure 5.6: SEM photograph of a diesel injector nozzle (Robert Bosch GmbH, 2016).



Figure 5.7: SEM photograph of a diesel injector nozzle (Robert Bosch GmbH, 2016).

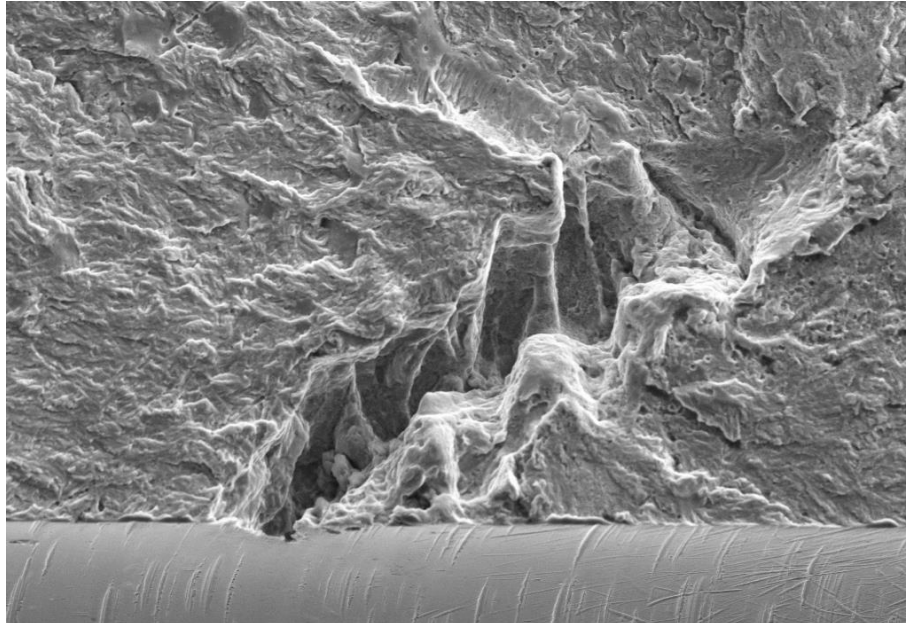


Figure 5.8: SEM photograph of a diesel injector nozzle (Robert Bosch GmbH, 2016).

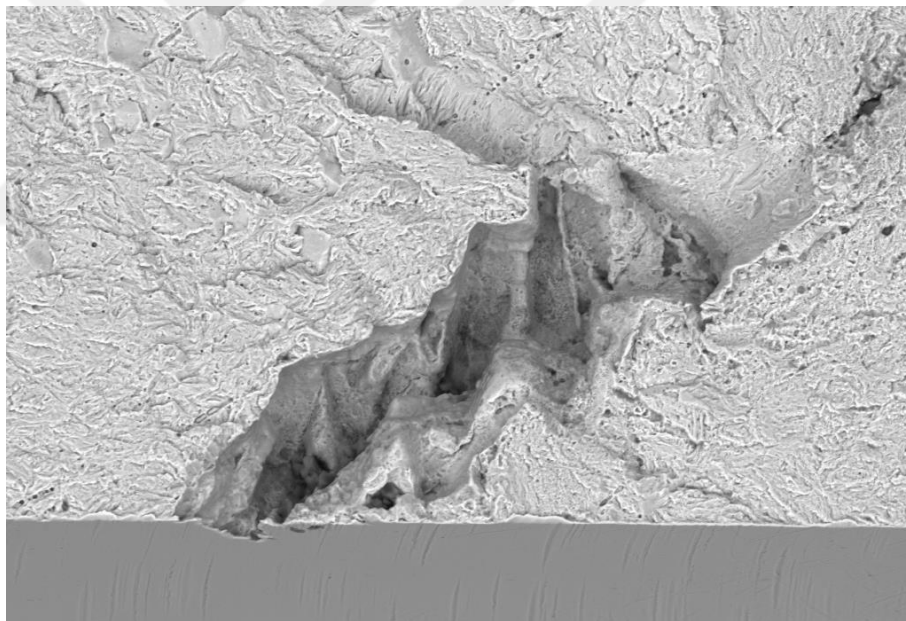


Figure 5.9: SEM photograph of a diesel injector nozzle (Robert Bosch GmbH, 2016).

The NMIs located on the seat region of the nozzle can cause relatively high failure probability when combined with factors such as a very heavy application, misuse or high stress on the seat. As the steel quality does not systematically differ from one nozzle design to the other, the load on the nozzle, and the nozzle tip design are the dominating factors for the robustness of the seat region.

As each customer complaint is a source of information to understand the problem, different aspects of each case are documented with details such as:

- Spray design
- Tip geometry
- Manufacturing date
- NMI type and dimensions
- NMI position
- Mileage
- Customer

With the accumulation of data from field complaints, the designs which are more prone to failures due to non-metallic inclusions are identified. The manufacturing date of the cracked nozzles are documented and it is seen that the number of nozzles delivered is coherent with the number of failed nozzles in field and therefore the failure mode is independent of manufacturing date, indicating that the problem does not come from a single steel melting batch (see Figure 5.10).



Figure 5.10: Field failure probability in a nozzle type in series manufacturing.

The position of the NMI on the seat region is critical, as this effects the distance of the NMI from the needle seat when the injector is closed and therefore the stress during the needle closing impact. When the NMI positions from the field cases are marked on

the injector nozzle body, it is seen that the critical positions causing nozzle tip cracks are between the needle seat and the sachel entrance (see Figure 5.11).

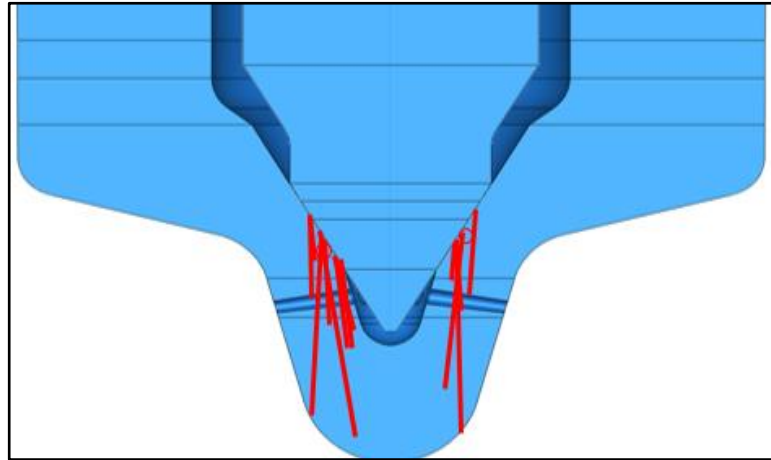


Figure 5.11: Positions of the NMIs which caused field failures.

Based on this, it can be told that a design delivering lower stress would decrease the NMI related failure probability in field. A definition combining the load and the tip design can therefore be used as a criteria for the criticality of the stresses on the seat and therefore the failure probability due to non-metallic inclusions. The load ratio of a nozzle is obtained by dividing the needle closing force to the steel volume located directly under the seat region shown in Figure 5.12 and is denoted by “F/A”. As this ratio gets smaller, the design gets more robust against the damaging effects of the field application.

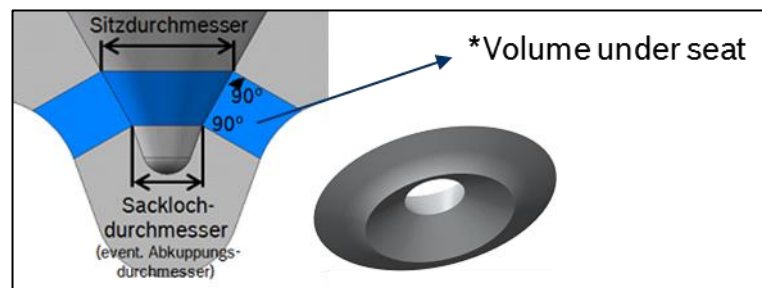


Figure 5.12: Definition of the volume withstanding the needle closing force.

The needle closing creates the main impact force acting on the needle seat region and therefore it is crucial to keep it in mind during the design process. The closing force differs from one injector generation to the other as the state of the art servo-hydraulic injectors are available with different maximum system pressure values. Although much smaller than differences between injector generations, peak nozzle pressure and

needle closing force values differ from one project to the other as well. In order to check whether a correlation between the load coefficient F/A and the field failure probability, the load coefficients of 4 nozzles types are calculated (see Table 5.1).

Table 5.1: Load coefficient comparison of different designs.

Design 1	Design 2	Design 3	Design 4
F/A: 43,76%	F/A: 48,62%	F/A: 100%	F/A: 83,71%

As a prerequisite for the correct calculation of the failure probability in field, the number of nozzles which fail and which did not or most probably will not fail need to be found.

All reported nozzle failure data is sorted based on the criteria given before and the number of failures per nozzle type relevant to non metallic inclusion is documented (see Figure 5.13).

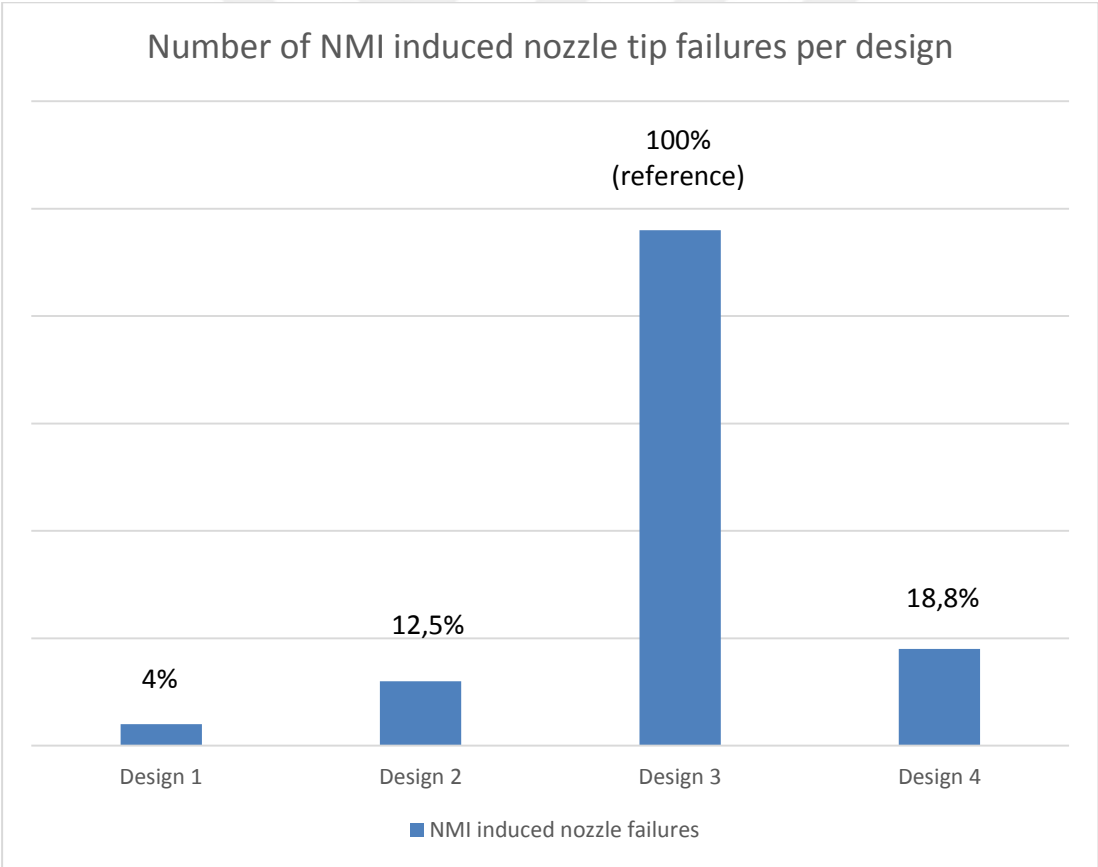


Figure 5.13: Number of NMI induced nozzle tip failures per design.

In order to calculate the number of parts without failure, the behaviour of NMI induced nozzle failures is analyzed. The mileage of the relevant failures are evaluated. As

shown in Figure 5.14, It is found that around 80% of the cracks occur within the first 20.000 kms and all parts failed from the nozzle tip have failed within the first 80.000 kms.

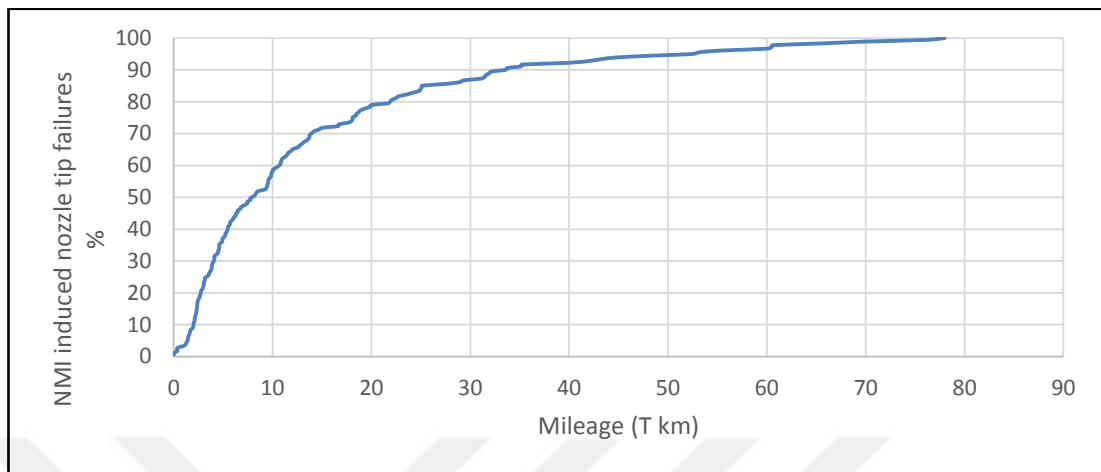


Figure 5.14: NMI induced nozzle tip failures percentage per mileage in field.

Based on the field release dates and the failure dates of the failed nozzles from these 4 designs, the usage statistics are prepared. The calculation of mileage per unit time shown in Figure 5.15 gives an idea about how much of the latest manufacturing volume should be ignored in order to accurately calculate the number of runout nozzles.

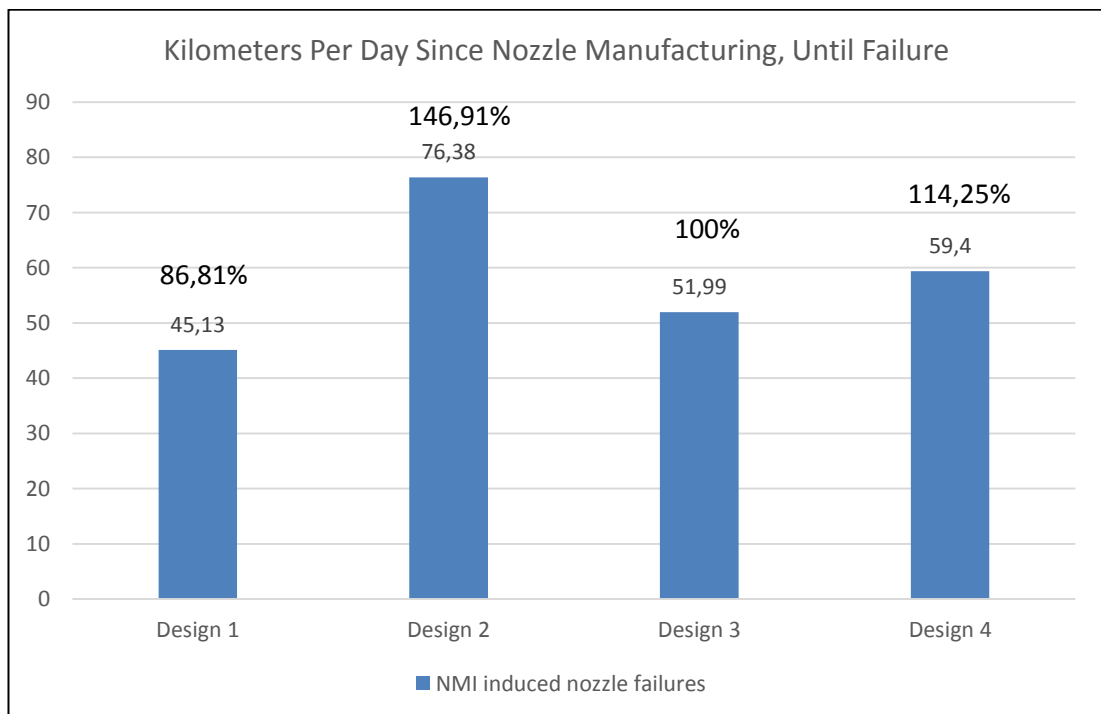


Figure 5.15: Daily mileage in field per design.

To be more conservative about the failure probability calculation, the number of nozzles which have not completed 80.000 km mileage in field, shown in Figure 5.16, are calculated and are excluded from the classification of runout nozzles.

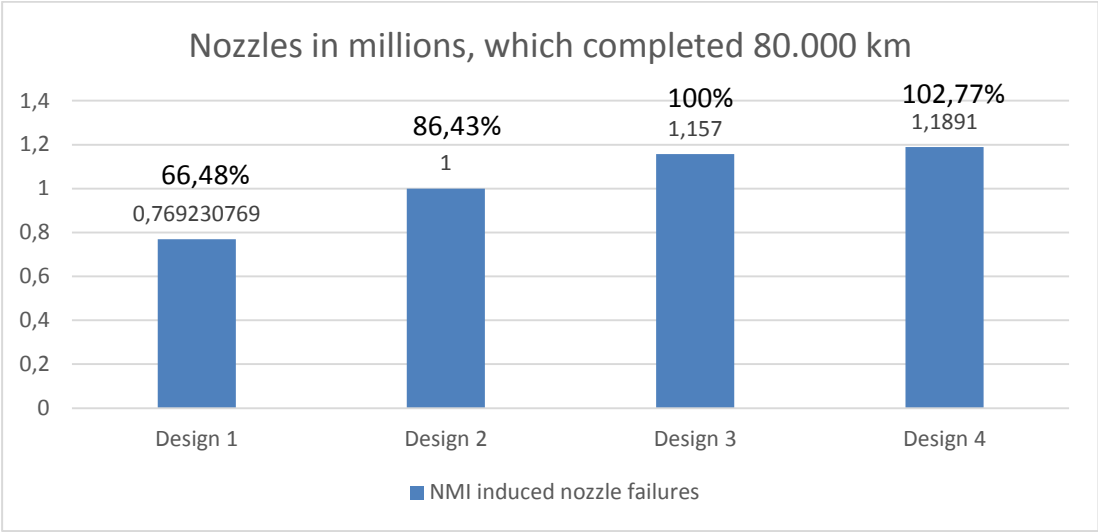


Figure 5.16: Comparison of number of runout nozzles per design.

The number of runout nozzles for each design is used as censored units in the Weibull analysis. Right censoring is applied in the analysis as the runout nozzles have completed at least 80.000 kms. For the Weibull analysis, the Minitab software (version 17) is used. With the aim of comparing and evaluating the results, both the maximum likelihood estimation and the least squares estimation are used. It is aimed to find whether a tangible correlation between the load coefficient of the deisgn and the Weibull distribution parameters, which can be used to plot the field reliability of another design after the first failures in field, or before field implementation.

6. RESULTS AND CONCLUSIONS

The Weibull plots for different designs were analyzed in order to evaluate the fit of the distribution to the data. The nozzle type with design #1 only had 2 nozzle failures in field which were relevant. The sample size for failed nozzles is very low and therefore an accurate estimation for the Weibull parameters is not possible. The distribution, based on least squares estimation and 2-parameter Weibull distribution, shows that for a long mileage, no failure would be observed, meaning the character resembles that of a 3-parameter Weibull distribution (see Figure 6.1). This is thought to be a side effect of a very small failed nozzle dataset.

Estimation based on few samples generally result in high shape parameter β and low characteristics life η (Abernethy et al, 1983). As the shape parameter cannot be estimated accurately based on the data of only 2 failed nozzles, evaluation based on experience of shape parameter with the other cases can be meaningful. This is method is called “Dauser shift”, shifting the Weibull plot with the same shape parameter β but a different scale parameter η , which satisfy the failure probability (Abernethy et al, 1983). As stated by Simpson in 1994, for the same root cause, the Weibull shape parameter can also be expected to stay the same.

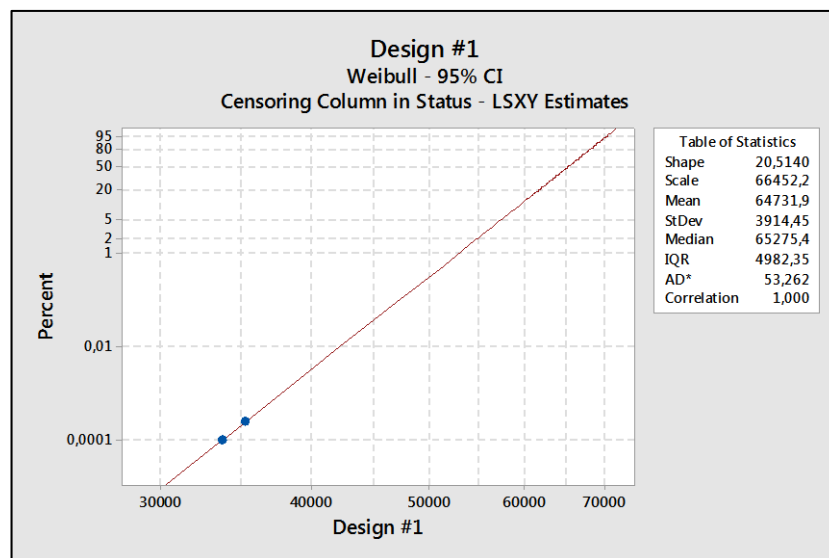


Figure 6.1: Weibull distribution plot for design #1.

The nozzle type with design #2 only had 4 nozzle failures in field which were relevant. While not as scarce as the failed nozzle data for design #1, the sample size is still low. The accuracy is therefore better and the data points mainly follow the Weibull plot with least squares estimation (see Figure 6.2).

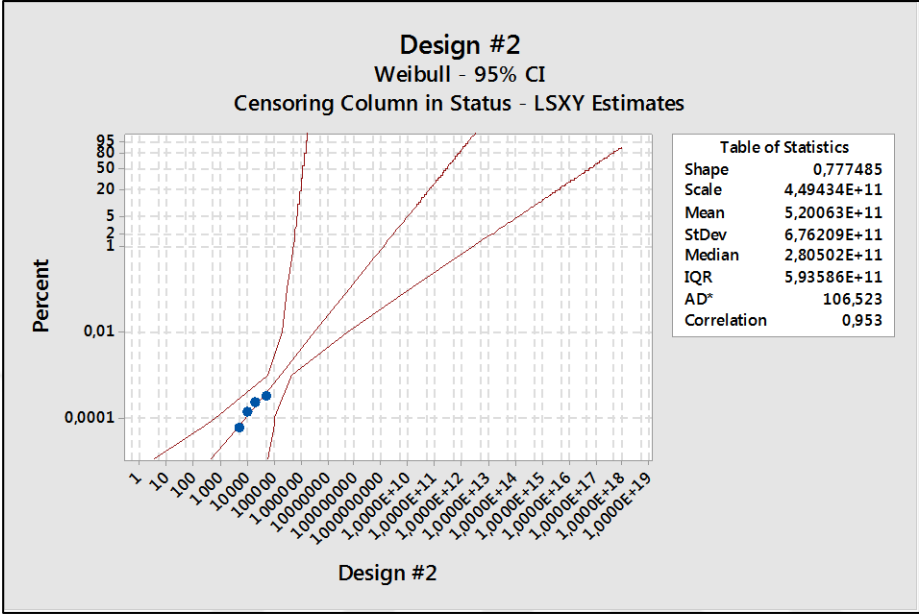


Figure 6.2: Weibull distribution plot for design #2.

The nozzle type with design #3 has a larger failed nozzle group and therefore the fit is Weibull distribution to the field situation is better. The data follows a straight line, which indicates that 2-parameter Weibull distribution is adequate (see Figure 6.3).

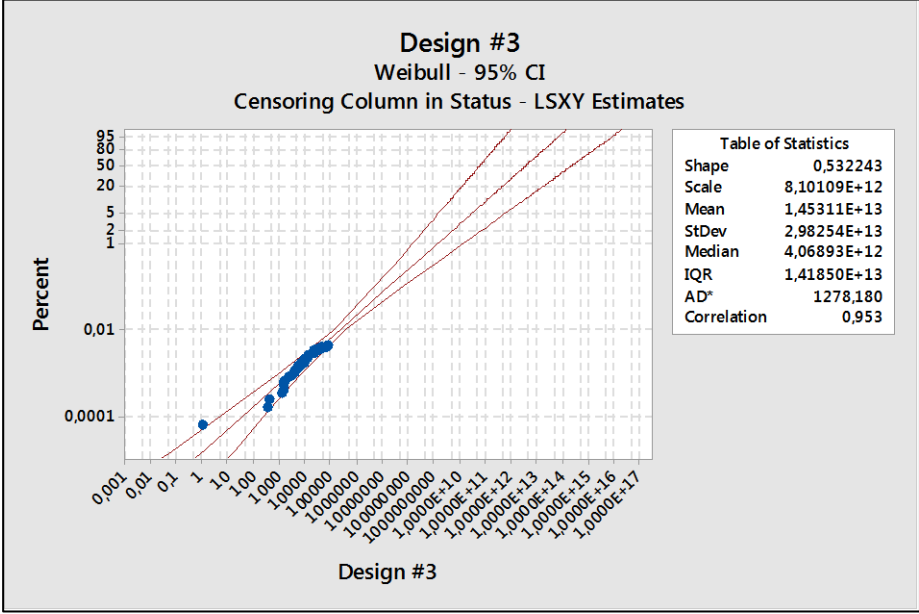


Figure 6.3: Weibull distribution plot for design #3.

The nozzle type with design #4 also has a larger failed nozzle group and therefore the fit of the Weibull distribution to the field situation is expected to be better compared to the data obtained from the field experience with design #1 and design #2. As shown in Figure 6.4, the data does not follow a straight line, which indicates that 2-parameter Weibull distribution is inadequate. The shape of the data points on the Weibull plot resembles a curve. This indicates that there can be failure free time, or in other words, a need for a location parameter (Abernethy et al, 1983).

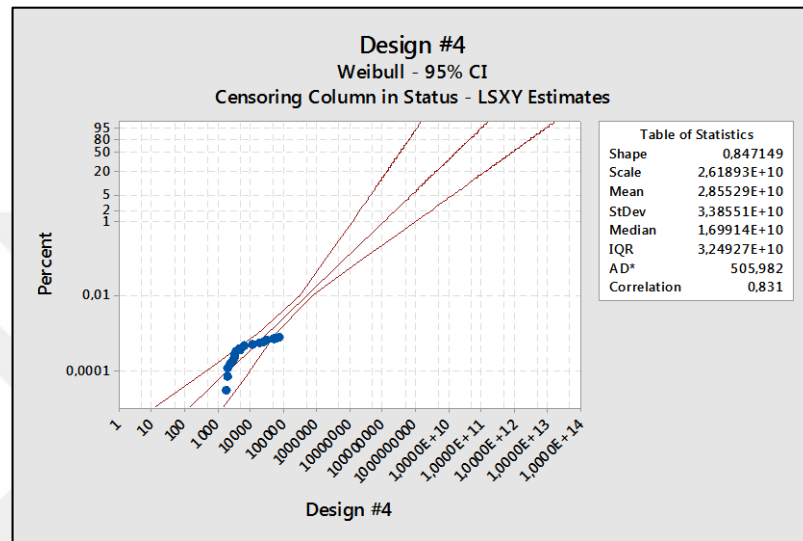


Figure 6.4: Weibull distribution plot for design #4.

The analysis is done once again, this time with 3-parameter Weibull distribution. With the addition of failure free time, the datapoints follow a straight line, which indicates that 3-parameter Weibull distribution is adequate (see Figure 6.5).

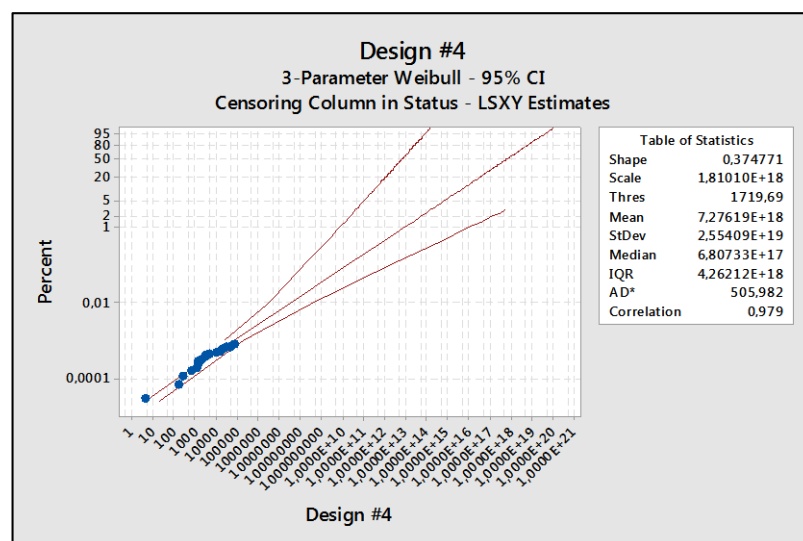


Figure 6.5: 3-parameter Weibull distribution plot for design #4.

After the parameter estimation is completed, the results are gathered in Table 6.1 for evaluation.

Table 6.1: Table of estimated Weibull distribution parameters.

Design #1	Design #2	Design #3	Design #4
F/A: 43,76%	F/A: 48,62%	F/A: 100%	F/A: 83,71%
$\beta = 20,51$	$\beta = 0,78$	$\beta = 0,53$	$\beta = 0,37$
$\eta = 66452,2$	$\eta = 4,49E+11$	$\eta = 8,10E+12$	$\eta = 1,81E+18$
$\gamma = \text{unnecessary}$	$\gamma = \text{unnecessary}$	$\gamma = \text{unnecessary}$	$\gamma = 1719,69$

It is seen that the shape parameter β and the scale parameter η does not change in a direct correlation with the load coefficient F/A. The results show that the shape parameter β is mainly smaller than unity, indicating an infant mortality problem. In order to further assess the situation, the failure probabilities of the nozzles for each design is calculated via the the formula:

$$\text{Field failure probability: } \frac{\text{Number of relevant failures}}{\text{Total number of relevant nozzles in field}} \quad (6.1)$$

The failure probability of each nozzle design is then plotted on the same graph with respect to the load coefficient (see Figure 6.6).

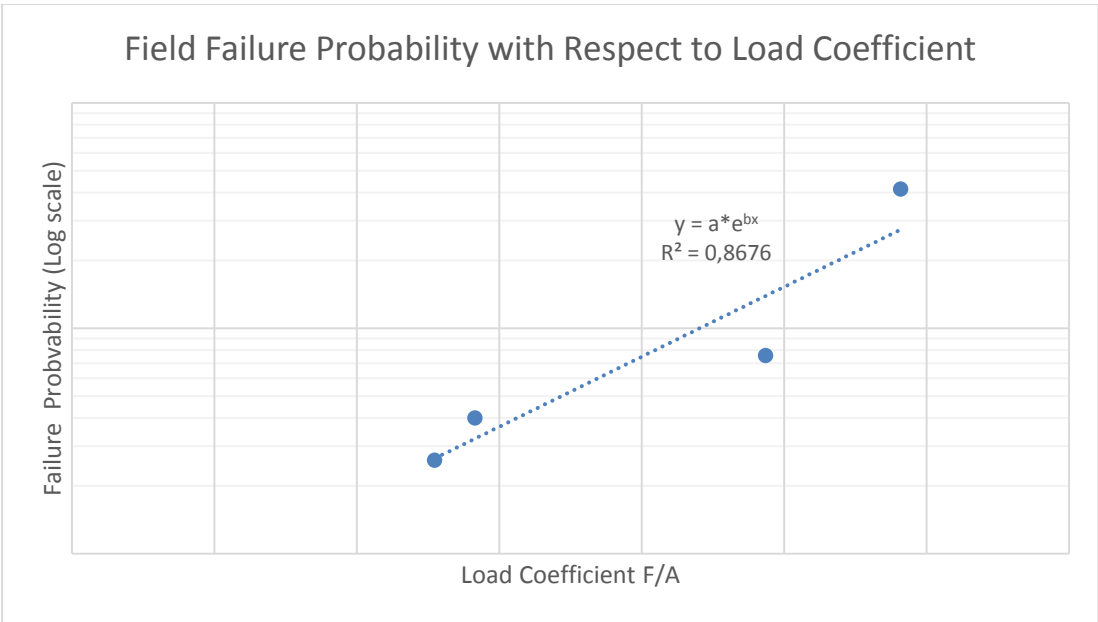


Figure 6.6: Field failure probability vs load coefficient F/A.

The graph indicates a correlation in the form of an exponential function, which can be used for NMI related nozzle tip failure probability estimation before the product is

released for series manufacturing, or for early actions after receiving customer quality complaints due to nozzle failures originating from non-metallic inclusions the seat region.

It is concluded that due to very few failures in field resulting in very small failure probability and hence scarce data related to failures, the parameters could not be estimated very accurately, as a results of which a direct correlation of Weibull parameters could not be found. However, the failure probability and the load coefficient of the designs compared in this study show an exponential correlation and therefore may indicate that given more data, the Weibull distribution could prove adequate to analyze non-metallic inclusion related injector nozzle tip failures seen in field.

In order to see the combined character from all designs, all failures from the four previously analyzed design variants were combined in one list and a 2 parameter Weibull analysis was performed. It is seen that the data does not follow a straight line, which indicates that 2-parameter Weibull distribution is once again not adequate. The shape of the data points shown on the Weibull plot resembles a curve, with some failures not complying with the general behaviour (see Figure 6.7).

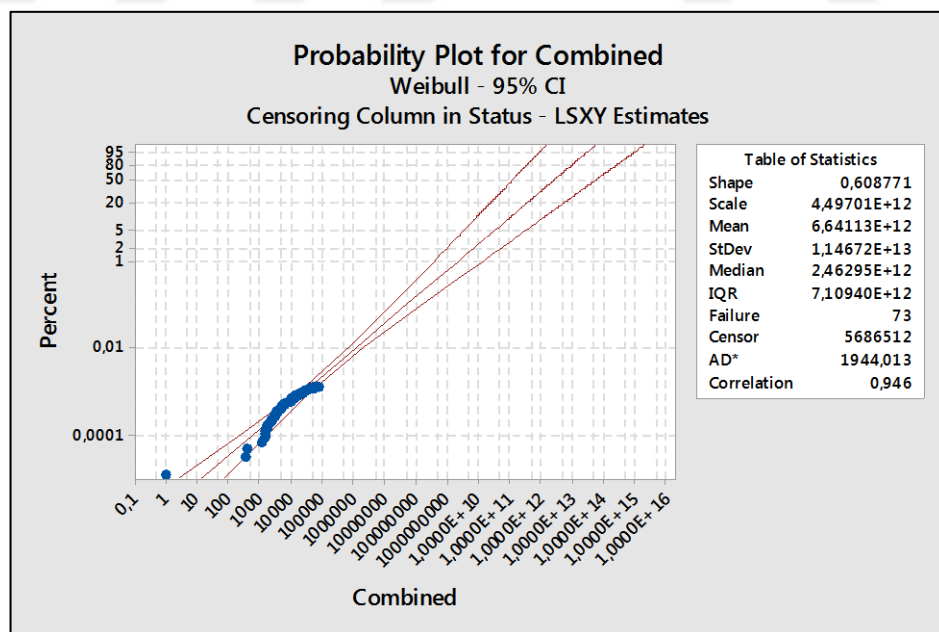


Figure 6.7: Weibull distribution plot for 4 variants combined.

The analysis is performed once again using 3-parameter Weibull distribution, and now with the non-compliant failures cancelled out from the evaluation. With the addition

of failure free time, the datapoints follow a straight line, which indicates that 3-parameter Weibull distribution is adequate, similar to the situation for Design #4 (see Figure 6.8).

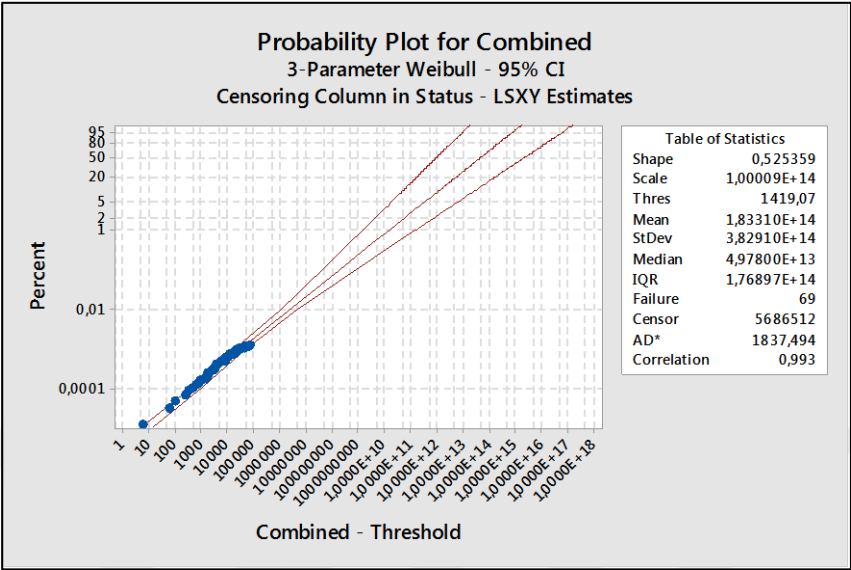


Figure 6.8: 3-parameter Weibull distribution plot for 4 variants combined.

To see whether the combined character will resemble that of a newer design, the results of another design, denoted by “Design #5” is analyzed. Similar to the other variant, the milage per day is calculated as 33,20 kilometers. The amount of nozzles which have not completed 80.000 kilometers in field are cancelled out. Using the field failure data and the number of runout nozzles as right censored parts, the Weibull distribution plot is prepared (see Figure 6.9).

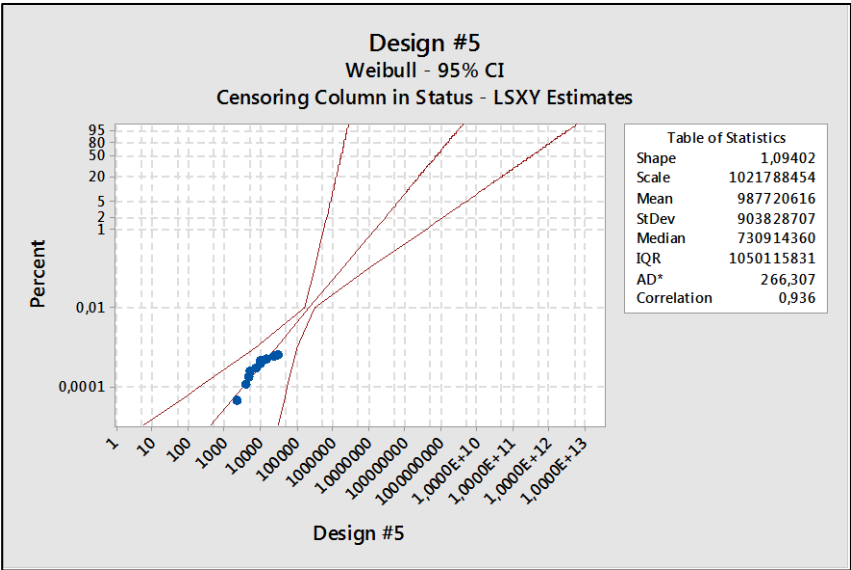


Figure 6.9: Weibull distribution plot for design #5.

The analysis is done once again, this time with 3-parameter Weibull distribution. With the addition of failure free time, the datapoints follow a straight line as also seen in the previous evaluation with 2-parameter Weibull distribution, but with higher correlation coefficient (see Figure 6.10).

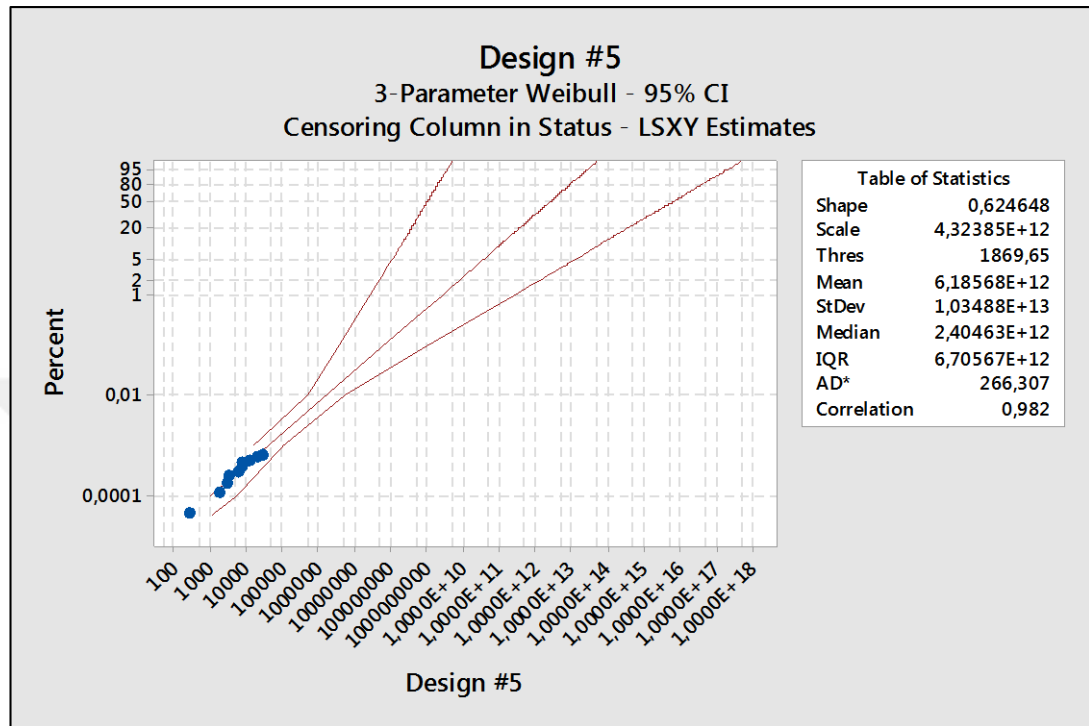


Figure 6.10: 3-parameter Weibull distribution plot for design #5.

Comparison and analysis of field data related to the first 4 designs combined and the 5th show that due to very few failures in field resulting in very small failure probability and hence scarce data related to failures, the parameters could not be estimated very accurately, as a result of which a direct prediction of Weibull parameters was not possible. However, the estimated shape factors for other designs combined and the 5th design do not show a very high variance, indicating that the Weibull distribution could prove adequate to analyze and predict non-metallic inclusion related injector nozzle tip failures seen in field.



REFERENCES

- Abernethy, R. B., Breneman, J. E., Medlin, C. H., & Reinman, G. L.** (1983). Weibull analysis handbook (No. PWA/GPD-FR-17579). PRATT AND WHITNEY WEST PALM BEACH FL GOVERNMENT PRODUCTS DIV.
- Çakır Zeytinoğlu, F.** (2009). Weibull Dağılımının Ölçek Ve Biçim Parametreleri İçin İstatistiksel Tahmin Yöntemlerinin Karşılaştırılması. *İstanbul Ticaret Üniversitesi Sosyal Bilimler Dergisi Yıl:8 Sayı:15* (pp. 73-87)
- Gusenbauer, C., Reiter, M., Kastner, J., & Klösch, G.** (2014). Detection of Non-Metallic Inclusions in Steel by X-ray Computed Tomography and After Fatigue Testing. In *Proceedings of European Conference on Non-Destructive Testing*.
- International Council on Clean Transportation** (2015). European vehicle market statistics. (Report Nr. 2015/16) Washington, DC: International Council on Clean Transportation Report.
- Miller, J. and Façanha, G.** (2014). The state of clean transport policy. Washington, DC: International Council on Clean Transportation Report.
- Murakami, Y.** (2002). *Metal fatigue: effects of small defects and nonmetallic inclusions*. Elsevier.)
- Murakami, Y.** (2012). Material defects as the basis of fatigue design. *International Journal of Fatigue*, 41, 2-10.
- Nakashima, J., & TOH, T.** (2013). Improvement of Continuously Cast Slabs by Decreasing Nonmetallic Inclusions. *Nippon steel technical report*, (104).
- Norm, D. I. N.** (1985). 50602: Metallographische Prüfverfahren; Mikroskopische Prüfung von Edelstählen auf nichtmetallische Einschlüsse mit Bildreihen. *Beuth, Berlin, Sept.*).
- Reif, K. (Ed.)**. (2012). *Klassische Diesel-Einspritzsysteme: Reiheneinspritzpumpen, Verteilereinspritzpumpen, Düsen, mechanische und elektronische Regler*. Springer-Verlag.
- Ren, Y., Wang, Y., Li, S., Zhang, L., Zuo, X., Lekakh, S. N., & Peaslee, K.** (2014). Detection of non-metallic inclusions in steel continuous casting billets. *Metallurgical and Materials Transactions B*, 45(4), 1291-1303.
- Warwick Manufacturing Group.** (2004). *The Use of Weibull in Defect Data Analysis*. Coventry: Warwick Manufacturing Group.

- Wintrich, T., Krüger, M., Naber, D., Zeh, D., Hinrichsen, C., Uhr, C., ... & Rapp, H.** (2017). Bosch common rail for passenger car/light duty–The first 20 years. In *17. Internationales Stuttgarter Symposium* (pp. 177-191). Springer Vieweg, Wiesbaden.
- Zhang, L., & Thomas, B. G.** (2003). Inclusions in continuous casting of steel. In *XXIV National Steelmaking Symposium, Morelia, Mich, Mexico* (Vol. 26, p. 28).
- Robert Bosch GmbH** (2014). Metallography Report (Report Nr. P_140211_m_001) Stuttgart : Robert Bosch GmbH Report.
- Robert Bosch GmbH** (2014). Metallography Report (Report Nr. P_140219_m_003) Stuttgart : Robert Bosch GmbH Report.
- Robert Bosch GmbH** (2015). *Diesel Injector Nozzle Training Slides* [PowerPoint slides].
- Robert Bosch GmbH** (2015). *Diesel Injector Nozzle Material Training Slides* [PowerPoint slides].
- Robert Bosch GmbH** (2016). Metallography Report (Report Nr. 1604183443) Bursa : Robert Bosch GmbH Report.
- Robert Bosch GmbH** (2017). *Diesel Injector Nozzle Engineering ITU Training Slides* [PowerPoint slides].
- Robert Bosch GmbH** (2017). *Diesel Injector Nozzle Fatigue Strength and Material Failures Training Slides* [PowerPoint slides].
- Robert Bosch GmbH** (2017). *Diesel Injector Nozzle Field Reliability Observation Slides* [PowerPoint slides].
- Simpson, F. M.** (1994). The Use of Weibull Analysis Methods in Assessing Field Failure Problems.
- Türkan, A.** (2007). *Güvenilirlik analizinde kullanılan istatistiksel dağılım modelleri.* (Yüksek lisans tezi). Çukurova Üniversitesi, Fen Bilimleri Enstitüsü, ADANA.
- Url-1** <<https://earthobservatory.nasa.gov/Features/GlobalWarming/page2.php>>, date of access: 01.10.2017.
- Url-2** <<https://www.mercedes-benz.com/de/mercedes-benz/classic/museum/mercedes-benz-260-d-pullman-limousine/>>, date of access: 01.10.2017.
- Url-3** <https://www.synthesisplatform.net/references/Life_Data_Analysis_Reference.pdf>, date of access: 01.10.2017.

CURRICULUM VITAE

Name Surname : İbrahim CİVANOĞLU
Place and Date of Birth : 09.05.1988 Istanbul
E-Mail : ibrahimcivanoglu@gmail.com

EDUCATION :

- **B.Sc.** : 2011, Istanbul Technical University, Faculty of Mechanical Engineering, Department of Mechanical Engineering
- **M.Sc.** : 2018, Istanbul Technical University, Faculty of Mechanical Engineering, Department of Mechanical Engineering, Automotive Engineering Programme

PROFESSIONAL EXPERIENCE AND REWARDS:

- 2011-Present Robert Bosch San ve Tic A.Ş. - Dizel Sistemler Ar-Ge Merkezi